TECHNICKÁ UNIVERZITA V LIBERCI
Fakulta textilní

Studium difuze alaptidu z nanovlákenných vrstev

Diplomová práce

Studijní program: N3106 – Textilní inženýrství
Studijní obor: 3106T018 – Netkané a nanovlákenné materiály

Autor práce: **Bc. Nikifor Asatiani**
Vedoucí práce: Ing. Petr Mikeš, Ph.D.

Liberec 2018

TECHNICAL UNIVERSITY OF LIBEREC
Faculty of Textile Engineering

Study of diffusion of alaptide from nanofibrous layers

Master thesis

Study programme: N3106 – Textile Engineering
Study branch: 3106T018 – Nonwoven and Nanomaterials

Author: **Bc. Nikifor Asatiani**
Supervisor: Ing. Petr Mikeš, Ph.D.

Liberec 2018

Technická univerzita v Liberci
Fakulta textilní
Akademický rok: **2017/2018**

ZADÁNÍ DIPLOMOVÉ PRÁCE

(PROJEKTU, UMĚLECKÉHO DÍLA, UMĚLECKÉHO VÝKONU)

Jméno a příjmení:	**Bc. Nikifor Asatiani**
Osobní číslo:	**T16000082**
Studijní program:	**N3106 Textilní inženýrství**
Studijní obor:	**Netkané a nanovlákenné materiály**
Název tématu:	**Studium difuze alaptidu z nanovlákenných vrstev**
Zadávající katedra:	**Katedra netkaných textilií a nanovlákenných materiálů**

Zásady pro vypracování:

1. Studium a analýza difuzní rovnice v cylindrických souřadnicích
2. Návrh a realizace experimentu umožňujícího integraci alaptidu do nanovlákených struktur
3. Vyhodnocení kinetiky uvolňování
4. Závěr a zhodnocení výsledků

Rozsah grafických prací: **dle potřeby dokumentace**

Rozsah pracovní zprávy: **40-60 dle potřeby**

Forma zpracování diplomové práce: **tištěná/elektronická**

Seznam odborné literatury:

1. Crank, J. (1975), The mathematics of diffusion, Clarendon Press Oxford.
2. Chasin, M. (1990), Biodegradable Polymers as Drug Delivery Systems, Taylor & Francis.
3. Kodíček, M., Valentová, O. and Hynek, R. (2015), Biochemie: chemický pohled na biologický svět, Praha: VŠCHT.
4. Siepman, J., Siegel, R.A., Rathbone, M.J. (2012), Fundamentals and Applications of Controlled Release Drug Delivery, Springer US.

Vedoucí diplomové práce: **Ing. Petr Mikeš, Ph.D.**
Katedra netkaných textilií a nanovlákenných materiálů

Datum zadání diplomové práce: **13. října 2017**

Termín odevzdání diplomové práce: **4. května 2018**

Technická univerzita v Liberci Fakulta textilní

L.S.

Ing. Jana Drašarová, Ph.D.
děkanka

prof. RNDr. David Lukáš, CSc.
vedoucí katedry

V Liberci dne 13. října 2017

Prohlášení

Byl jsem seznámen s tím, že na mou diplomovou práci se plně vztahuje zákon č. 121/2000 Sb., o právu autorském, zejména § 60 – školní dílo.

Beru na vědomí, že Technická univerzita v Liberci (TUL) nezasahuje do mých autorských práv užitím mé diplomové práce pro vnitřní potřebu TUL.

Užiji-li diplomovou práci nebo poskytnu-li licenci k jejímu využití, jsem si vědom povinnosti informovat o této skutečnosti TUL; v tomto případě má TUL právo ode mne požadovat úhradu nákladů, které vynaložila na vytvoření díla, až do jejich skutečné výše.

Diplomovou práci jsem vypracoval samostatně s použitím uvedené literatury a na základě konzultací s vedoucím mé diplomové práce a konzultantem.

Současně čestně prohlašuji, že tištěná verze práce se shoduje s elektronickou verzí, vloženou do IS STAG.

Datum:

Podpis:

Acknowledgement

First of all, I wish to express my sincere gratitude to my supervisor Ing. Petr Mikeš, Ph.D. for all his support, guidance and patience. I would also like to thank the members of the Department of Nonwovens and Nanofibrous materials, Professor David Lukáš, Ing. Věra Jenčová, Ph.D., for their valuable suggestions and comments which helped to improve the thesis, RNDr. Jana Horáková Ph.D for a great help with *in vitro* tests of cytotoxicity. I would also like to thank Mgr. Vít Novotný for his invaluable assistance with the GPC analysis of the samples. I am also grateful to my family for all their emotional and financial support. Finally, I would like to acknowledge the assistance provided by the Research Infrastructures NanoEnviCz (Project No. LM2015073) supported by the Ministry of Education, Youth and Sports of the Czech Republic.

Abstract

There is a lack of studies related to drug release kinetics from electrospun fibrous structures nowadays. Indeed, even less studies try to verify to compare experimental data with mathematic models. This study investigated the effects of drug loading and sterilization technics on release kinetics of alaptide from polycaprolactone (PCL) electrospun nanofibrous layers. With the increasing drug loading increased hydrophilicity of the layers and decreased the fiber diameters. The release of alaptide was quantified using GPC. All the release profiles were found to be biphasic, consisting of significant initial burst release and further slow sustained release. The release kinetics were significantly dependent on the initial drug loading, sterilization with EtO did not remarkably affect the release. Fitting of data into mathematical models was complicated due to biphasic character of the release profiles. The study demonstrated successful fabrication of drug-loaded nanofibrous layers, which were able to provide sustained release of alaptide at least for 14 days.

Key words: drug release kinetics, alaptide, diffusion equation, polycaprolactone

Abstrakt

V dnešní době je nedostatek studií zabývajících kinetikou uvolňování léčiv z elektrostatický zvlákněných struktur. Ve skutečnosti, ještě méně studií se snaží porovnávat experimentální data s matematickými modely. Tato práce se zabývala studiem vlivu počátečního množství inkorporovaného léčiva a sterilizačních metod na kinetiku uvolňování alaptidu z elektrostaticky zvlákněných vláken polykaprolaktonu (PCL). Se zvyšující se dávkou alaptidu rostla hydrofilnost vrstev a snižovaly se průměry vláken. Ke kvantifikaci uvolňování byla použita metoda GPC. Veškeré průběhy byly dvoufázové, se značným počátečním nárazovým uvolněním a dále pokračovala zpomaleným uvolněním. Kinetika uvolnění byla značně závislá na dávce alaptidu. Sterilizace EtO nezpůsobila žádné patrné změny kinetiky uvolňování. Fitování dosažených dat bylo komplikováno dvoufázovou povahou uvolňování. Práce názorně ukázala úspěšnou výrobu nanovlákenných vrstev, schopných uvolňovat léčivo po dobu minimálně 14 dní.

Klíčová slova: kinetika uvolňování léčiv, alaptid, difuzní rovnice, polykaprolakton

Table of contents

List of abbreviations

Ala	Alaptide
CI	Confidence interval
DDS	Drug delivery system
DMEM	Dulbecco's Modified Eagle Medium
EtO	Ethylene oxide
EtOH	Ethanol
GPC	Gel permeation chromatography
MIF	Melanocyte-stimulating hormone release-inhibiting factor
Mw	Molecular weight
PBS	Phosphate-buffered saline
PCL	Polycaprolactone
SD	Standard deviation
SEM	Scanning electron microscope
SLS	Sodium lauryl sulphate
THF	Tetrahydrofuran

Introduction

Nowadays there is a great demand in a searching of new methods of drug delivery, which involves modification of existing methods and as well as development of new devices. Increasing amount of controlled-release systems have been developed and designed lately to enhance drug therapy. A controlled-delivery system allows to reduce the frequency of dosing, to minimize the fluctuation of drug concentration in plasma and to generally increase effectiveness of the drug by a) targeting the site of action, b) maintaining drug level within a desired range, i.e. high enough to have a therapeutic effect and low enough to be non-toxic (Siepmann, Siegel and Rathbone, 2012). Despite the fact, there are hundreds of commercially successful products based on the controlled release rate of the drug, there are only a few main mechanisms by which a release rate is controlled, e.g. diffusion, osmosis, erosion (Hillery, Lloyd and Swarbrick, 2001). Individual mechanisms are dependent on particular application and design of drug releasing systems, however usually more than one mechanism operate at the same time during delivery process (Siepmann, Siegel and Rathbone, 2012). Indeed, diffusion is a dominant process within most of controlled-release systems. In case of diffusion-controlled release system, drug must diffuse through a polymer matrix or a membrane in order to be released. Such devices do not usually perform zero-order release profile as the particles on the surface release fast involving a *burst release*, whereas for the particles close to the center of fiber it takes longer to migrate towards the surface. This delay leads to decreasing rate of drug release over time (Hillery, Lloyd and Swarbrick, 2001).

The choice of a sterilization technique of biodegradable scaffolds or drug-delivery devices is, undoubtedly, a key issue, as biodegradable polymers, such as polycaprolactone, used in tissue engineering have specific properties, e.g. low melting point, and cannot be proceeded as conventional polymers, e.g. sterilization by autoclaving (Horakova *et al.*, 2017). Although no perfect sterilization technique exists, ethylene oxide (EtO) sterilization is suitable for most low melting polymers. Sterilization using ethanol (EtOH), despite it involves biochemical and morphological changes of a scaffold, is also often used due to its low cost, quickness and low temperature required for this technique (Dai et al., 2016).

Unfortunately, there is a lack of studies related to drug release kinetics from electrospun nanofibrous structures. Indeed, even less studies today try to verify and to compare experimentally obtained data with mathematical models. As note M. Grassi

and G. Grassi (2014) in their review on mathematical models application in DDS, the initial problem concerning the ability of mathematical modeling to accurately describe the experimental data was replaced with the issue of reliable prediction of drug releases on the basis of an adequate number of experimental data. These predictions of drug release, on the basis of initial parameters, e.g. diffusion coefficient, drug loading, etc., are necessary in development of a field of "personalized medicine" (Grassi and Grassi, 2014), which could provide each patient an unique therapy.

Generally, the aim of this study was to investigate drug release kinetics from a monolith diffusion-controlled device, represented by particles of alaptide homogeneously distributed within polycaprolatone nanofibrous layer. Particularly, an effect of three different initial drug loading was examined. Moreover, an effect of sterilization by ethylene oxide on release kinetics of alaptide and on morphology of nanofibrous layers was studied; an effect of sterilization with ethanol on morphology of electrospun nanofibrous structures was investigated as well. Finally, an attempt to establish a mathematical model for prediction of release kinetics of examined drug delivery system, proceeding from experimentally obtained data and on the basis of the solution of the diffusion equation, was made.

1 Literature review

1.1 Current state of electrospun-based controlled drug delivery systems

Development and investigation of electrospun-based drug delivery systems (DDS) are comparatively new issue. As a first publication on this topic is assumed an article by Kenawi et al. (2002), which describes a release kinetics of tetracycline hydrochloride as a model drug from electrospun layers of either poly(lactic acid) or poly(ethylene- co-vinyl acetate) and its 50/50 blend. The study showed that drug can be successfully incorporated in nanofibers with 90% loading efficiency just by solubilizing the drug into the polymer solution.

Undoubtedly, an interest in controlled DDS based on electrospun nanofibrous structures significantly grew within last 16 years since Kenawi's study (2002) had been published. However, as was already mentioned in introduction, there is still only a limited number of publications related to this issue. For instance, in a broad review article by Dash and Konkimalla (2012) on polycaprolactone-based formulations for DDS, there is an impressive list of studies considering polycaprolactone-based microspheres and nanoparticles, while list of studies on electrospun fibrous structures as a drug carriers is considerably smaller. Likewise, Deng-Guang Yu (2009) mentions a lack of research reports on this problem in his review.

Indeed, among a handful of articles on electrospun-based DDS, one can distinguish three major trends: a) articles which focus primarily on fabrication and characterization of a drug-carrier, subsequently providing only general information on release behavior of a model drug (e.g. Jiang *et al.*, 2005); b) articles describing release kinetics in detail without comprehensive mathematical assessment (e.g. Hrib *et al.*, 2015); c) articles concerning simulations and a development of new mathematical models (e.g. Kojic *et al.*, 2017). Furthermore, only minority of the publications provide both experimental and numerical evaluation of drug release kinetics, comparing experimentally obtained data with mathematical models, e.g. recent publication by Zahida Sultanova *et al.* (2016) on controlled ampicillin release from coaxially electrospun PCL nanofibers, or the article by P.Nakielski *et al.* (2015) on numerical assessment of drug release from electrospun nanofibrous layer to brain tissue and also their research (2013) on modeling of drug release from nanofibers-based materials, on the basis of data experimentally obtained in their labs. It is worth mentioning, that there are also attempts to develop a new model on

the basis of already published data as, for instance, in the recent study by Petlin *et al.*, (2017). Petlin *et al.* developed a mathematical model for prediction of drug release rates on the basis of fiber diameter distribution using SEM images obtained from publications. The study also demonstrated that the presence of fibers with different diameters can significantly affect release rates and the burst effect.

In view of the foregoing, there is no doubt that investigation of electrospun-based DDS is a quite wide field and to date there are many challenges for researches to be met. Among the main unsolved problems, Yu *et al.* (2009) mentions the problem of drug loading and related initial burst release, the residual of organic solvent, the stability of incorporated compounds and lack of *in vivo* studies. Thus, the current study is designed in a such way that it attempts to combine the experience of the previous studies in this field and to fill the gaps of understanding of the basics of release kinetics and the factors (sterilization and its residuals, pretreatment of the delivery devices, etc.) affecting this release. In particular, the emphasis was made not only on investigation of the influence of drug loading on its release kinetics, but also on comparing the obtained data with existing mathematical models, as opposed to e.g. similar study by Luong-Van *et al.* (2006), where in like manner, heparin release from electrospun nanofibrous DDS was investigated, however no mathematical assessment was provided.

1.2 Diffusion

1.2.1 The diffusion process.

The Latin word ‘diffundere’ means ‘to spread out’ (Mehrer and Stolwijk, 2009). John Crank (1975), in his famous book “Mathematics of diffusion”, succinctly describes diffusion as a process by which matter is transported from one part of the system to another due to random molecular motion, i.e. so called Brownian motion. Brownian motion generally qualifies a *random-walk* of microscopic particles in suspension in a fluid and it is named after a Scottish botanist Robert Brown, who described the chaotic movement of pollen grain particles on a surface of a fluid in 1828 (Brown, 1828). Quite often, in popular books, e.g. “One two three… Infinity” by George Gamow (1988), random-walk is compared to a “wanderings of a drunk-sailor” (see Fig. 1). However, the mathematical form of Brownian motion was presented more than a half century later, in 1905, by German-Jewish physic Albert Einstein (Einstein, 1905). Einstein expressed a macroscopic quantity, i.e. diffusivity, in terms of microscopic laws, i.e. elementary jumps of atoms and molecules. In other words, A. Einstein created a bridge between the laws of microscopic and macroscopic world. He was the first to realize that trajectories of particles motion are such that their velocity is irrelevant. Instead, the main quantity is the mean square displacement of particles in a given time, i.e. $<R^2(t)>$ (Philibert, 2005). Indeed, in a dilute solution the motion of individual molecules is not only random but also independent of other molecules in the system. Despite the mean-square distance traveled by a single molecule within a given time period can be calculated using a *random-walk* model, one is not able to determine direction of the motion in this time.

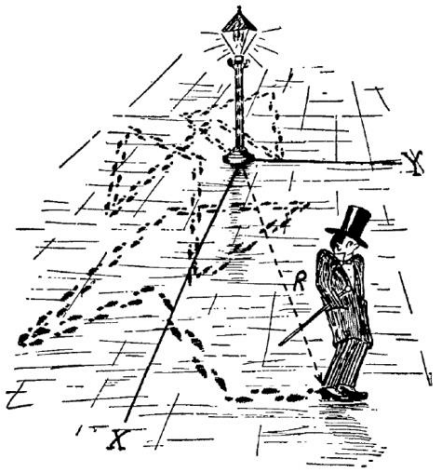

Fig. 1 Illustration of a random walk as wanderings of a drunk sailor (Gamow, 1988)

Even though individual molecules do not have any preferred direction of motion, the transport of diffusing matter is always directed from the regions with higher concentration of its molecules to regions with lower concentrations. J. Crank (1975) explains this phenomena considering a horizontal section in the system, i.e. iodine solution, and two thin equal elements of volume just below and above this given section. Next J. Crank states, that in a given time, an average fraction of iodine molecules crossing the section from the lower element will be equal to an average fraction of iodine molecules crossing the volume from the upper element. Hence, random motions result in a net transfer from the lower side of the section to the upper one simply due to a greater amount of iodine molecules in the lower element.

Diffusion process plays a significant part in majority of controlled-release DDS. Even though, the release kinetics of a drug is dependent on several concurrent factors, including swelling of a matrix, drug dissolution etc. Indeed, J. Siepmann *et al*, (2012) emphasizes that generally the slowest process is dominant should be considered. Then, J. Siepman *et al.* provides an example of rapid drug dissolution followed by slow diffusion of a drug through a polymer matrix. It is important to mention, that if degradation of a matrix starts after a whole content of a drug is completely released (which could correspond to a delivery device investigated in this diploma thesis), then degradation factor is irrelevant and should not be involved in mathematical model describing release kinetics. Different mathematical models used to quantify release rate of a drug are discussed in the section 1.3.2.

In this study, diffusion was assumed to be the dominant release mechanism, as within experiment time, i.e. 14 days, polycaprolactone degradation effect is negligible (Ravi Kumar, 2016). The same assumption on basis of experimentally obtained data was reported earlier by Luong-Van *et. al*. con (2006) in study of heparin release from PCL electrospun nanofibers.

1.2.2 The diffusion equation.

There are two famous ways how to derive diffusion equation – first is so-called random walk approach and the second approach via the First and the Second Adolf Fick's laws. Detailed derivation of the diffusion equation in Cartesian coordinates from Fick's laws is described by Crank (1975), nevertheless in this chapter only few general steps of derivation process are provided. The random walk approach is briefly described in next section.

Fick's laws

Adolf Fick (1855) was the first who described diffusion phenomenon in a quantitative way. Fick developed a mathematical framework using an analogy between two processes – diffusion and heat conduction, which was described by Fourier some years earlier, in 1822. As transfer of heat by conduction is also caused by random molecular motion, the mathematical conception of diffusion in isotropic media is based on assumption that the rate of transfer the diffusing matter through the unit of area of a section is proportional to the concentration gradient measured normal to the section, i.e.:

$$\Gamma = -\mathrm{D}\boldsymbol{\nabla}\mathrm{u}(\mathbf{r}) \qquad (1)$$

The equation (1) is what is called Fick's First law, where Γ is the flux of the diffusing material, D the diffusion coefficient, u(r) concentration of the diffusing substance at location r=(x, y, z), $\boldsymbol{\nabla} u(\boldsymbol{r}, t)$ is called the gradient of the concentration along the axis. If the flux, Γ, and the concentration, u, are expressed using the same unit of quantity, for instance gram, then diffusion coefficient, D, does not depend on the unit and has units of cm^2/s (Gurevich, 2008; Karimi, 2011).

The negative sign in the equation (1) denotes the fact, that diffusion proceeds in the opposite direction of concentration gradient, i.e. direction of decreasing concentration. Sometimes it is possible to assume D as a constant, e.g. diffusion in dilute solutions; otherwise, e.g. diffusion in high polymers, it significantly depends on concentration (Crank, 1975).

Whereas the first law can be directly applied for the case when concentration does not depend on time, i.e. steady state, for unsteady state Fick's Second law is used. This fundamental differential equation of diffusion can be derived from the equation (1) combining with the differential form of mass conservation law (or continuity equation),

which states that density fluctuations in any locations of the system is due to inflow and outflow of material into and out of that part of the system:

$$\frac{\partial \mathrm{u}}{\partial \mathrm{t}} = \nabla \cdot \Gamma = 0 \tag{2}$$

Substituting equation (1) for Γ in equation (2) gives:

$$\frac{\partial \mathrm{u(r,t)}}{\partial \mathrm{t}} = \nabla \cdot (D(u(r,t),r)\nabla u(r,t)) \tag{3}$$

If the coefficient D is constant, then equation (3) reduces simply to the following form:

$$\frac{\partial \mathrm{u(r,t)}}{\partial \mathrm{t}} = D\Delta u(r,t) \tag{4}$$

Where Δ denotes the Laplace operator. The equation (4) describes the diffusion process with respect to the time, t, and usually is referred to as Fick's second law, the diffusion equation or the heat equation as it also describes the spread of a heat in a given part of a system with respect to time (Crank, 1975; Gurevich, 2008; Karimi, 2011).

Random-walk approach

First of all, Albert Einstein found a relation between the diffusion coefficient of particles in suspension in a liquid, *D*, and the viscosity of solvent, η. Using an extension of *Stokes* friction force, $6\pi\eta r$, to solute molecules of a given radius, *r*, Einstein achieved the following:

$$\mathrm{D} = \frac{R_g T}{N_A} \frac{1}{6\pi\eta r} \tag{5}$$

Here R_g and N_A are, respectively, the ideal gas constant and the Avogadro constant. The obtained equation (5) is usually referred to as *Stokes-Einstein* relation. Secondly, A. Einstein considered successive positions of the particles at a given time interval, τ, on the assumption that τ is small enough and that the individual particles move independently on the movement of other particles. Then, the total displacement, *R*, of individual particles during time *t*, can be expressed as a sum of many intermediate displacements r_i:

$$\mathrm{R} = \sum r_i \tag{6}$$

As for a truly random walk (in case of the absence of any external forces) total displacement *R* equals zero, the square mean displacement, i.e. $<R^2(t)>$, is an appropriate quantity. As a result, Einstein derives a relation between the mean-square displacement, diffusivity and time, that is consistent with the second Fick's however with the diffusion coefficient being defined on a microscopic basis, i.e.:

$$D = \frac{1}{2\tau} < \Delta^2 > \tag{7}$$

Here Δ denotes a displacement of particles at a given time along a given direction.
In three dimensions, Einstein's equation can be written as follows:

$$< R^2 >= 6Dt \tag{8}$$

As was mentioned in the section 1.2.1, the relation (8), „built a bridge" between microscopic quantity, i.e. diffusivity, and a macroscopic quantity, i.e. mean displacement (Philibert, 2005; Mehrer and Stolwijk, 2009).

1.2.3 Solution of the diffusion equation.

There are several methods to obtain general solutions for the diffusion equation for a various initial and boundary conditions on assumption of constant diffusion coefficient. Generally, these solutions are obtained in two forms. The first deals with series of error functions and is more suitable for numerical evaluation at small times, e.g. initial stages of diffusion process. The second form is usually applied for a long-time period of diffusion as it deals with trigonometrical series (or series of Bessel function in case of cylindrical geometry) (Crank, 1975). Bessel functions are solutions of Bessel equation, i.e. $\frac{d^2y(x)}{dx^2} + \frac{1}{x}\frac{dy(x)}{dx} + \frac{x^2-v^2}{x^2}y(x) = 0$, and similarly as sines and cosines they appear in problems related to wave propagation (Caretto, 2016).

The next two chapters will illustrate basic steps for *analytical* and *numerical* solutions of one-dimensional diffusion problem.

Analytical solution

A large number of analytical solutions of Fick's second law of diffusion for different geometries and initial boundary conditions can be found in book "Mathematics of diffusion" (Crank, 1975).

In the following two sections, basic solution process in one-dimensional Cartesian and Cylindrical coordinates is provided.

Cartesian coordinates

Let us now consider an initial value problem for the diffusion equation (4) for an insulated fiber (see Fig. 2) in one dimension, i.e.:

$$\frac{\partial \mathrm{u(x,t)}}{\partial \mathrm{t}} = D\frac{\partial^2 \mathrm{u}(x,t)}{\partial x^2} \tag{9}$$

We also assume that the concentration is the same over each cross-section perpendicular to the fiber's axis. So, the general problem is to determine the concentration at each point within the fiber over time. Moreover, solution must satisfy initial and boundary conditions. For a fiber of diameter R, the spatial coordinated will be represented by x within closed interval $[0, R]$. A function $f(x)$ for $\forall x \in [0, R]$ denoting the initial concentration along the fiber radius provides the initial condition:

$$\mathrm{u(x,0) = f(x)}, \qquad \forall \mathrm{x} \in [0, \mathrm{R}] \tag{10}$$

Dirichlet boundary conditions provide zero flux conditions at fiber's surface:

$$\mathrm{u(0,t) = u(L,t)}, \qquad \forall \mathrm{t} > 0 \tag{11}$$

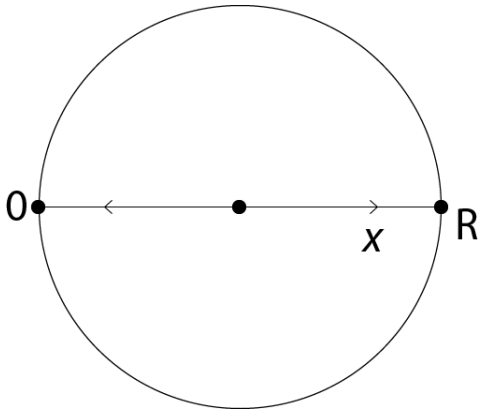

Fig. 2 Schematic illustration of the coordinate system for one-dimensional diffusion of matter from fiber's center to its boundaries; circle denotes cross-section of a fiber of diameter R;

As was mentioned before, there are several approaches to the solution of the diffusion equation, e.g. method of reflection and superposition; method of the Laplace transform (Crank, 1975). Despite this, the following text briefly provides basic solution steps using standard method of separation of variables, whose detailed description can be found in book by Chicone (2012) and also in chapter by Larry Caretto (2016). Firstly, we assume

that the variables are separable, so that we can attempt to find nontrivial solution for the equation by splitting concentration function, u, into two functions:

$$u(x,t) = X(x)T(t) \tag{12}$$

Where T(t) is a function of time only and X(x) is a function of distance only.

Substituting the following result to the initial equation (9) and then dividing both parts by the product $DX(x)T(t)$ we obtain the following:

$$\frac{1}{D}\frac{T'(t)}{T(t)} = \frac{X''(x)}{X(x)} = -\lambda \tag{13}$$

Since the right-hand side depends only on x and the left-hand side only on t, both sides are equal to some constant value $-\lambda$ (negative sign is chosen for convenience reasons), which gives us a system of two ordinary differential equations to solve:

$$X''(x) + \lambda X(x) = 0 \tag{14}$$

$$T'(t) + D\lambda T(t) = 0 \tag{15}$$

Solving the first equation for distance dependable function, X(x), which can be easily solved for each of the cases ($\lambda < 0,\ \lambda = 0$ or $\lambda > 0$), one has to take into consideration the boundary conditions (10) and (11). Only for $\lambda > 0$ it is possible to obtain satisfying nontrivial solution, i.e.:

$$X_n(x) = C_n \, sin\left(\frac{\pi n}{R}x\right), \quad n = 1,2 \ldots \tag{16}$$

Where n is an integer. The $sin\left(\frac{\pi n}{R}x\right)$ are a complete set of orthogonal eigenfunctions on the interval $0 \leq x \leq R$. The profiles of eigenfunctions for the first five values of n are depicted in Fig. 3.

The second equation for the T(t) function becomes:

$$T_n(t) = B_n \, exp\left(-D(\frac{\pi n}{R})^2 t\right) \tag{17}$$

where Bn is a constant.

Combination of these two solutions leads to the particular solutions of the initial equation (9):

$$u_n(x,t) = A_n sin\left(\frac{\pi n}{R}x\right) exp\left(-D\left(\frac{\pi n}{R}\right)^2 t\right) \qquad (18)$$

Where An is an unknown constant. These particular solutions represent sinusoidal distributions of the concentration, u, which attenuate over time. Also, it is important to mention that a value $\sqrt{\lambda_n} = \frac{\pi n}{R}$ is usually called wavenumber. It is evident that an argument of sine function in (18) represents multiplication of wavenumber $\frac{\pi n}{R}$ and coordinate x. Thus, λ_n corresponds to "oscillation frequency" or "level of fluctuations" of the concentration, *u*, in space. In like manner, one can consider a value $\Lambda_n = \frac{2\pi}{\sqrt{\lambda_n}}$ as a "period" of fluctuations of the concentration, u, with respect space coordinate, r (Самарский and Тихонов, 1999). In short, $\Lambda_n = \frac{2\pi}{\sqrt{\lambda_n}}$ is wavelength of sine functions, representing eigenvalue for u_n (see Fig. 3). The bigger the value of n, the smaller the period of sine wave in space (see Fig. 3) and also the faster it attenuates (due to $\exp\left(-D\left(\frac{\pi n}{R}\right)^2 t\right)$ factor).

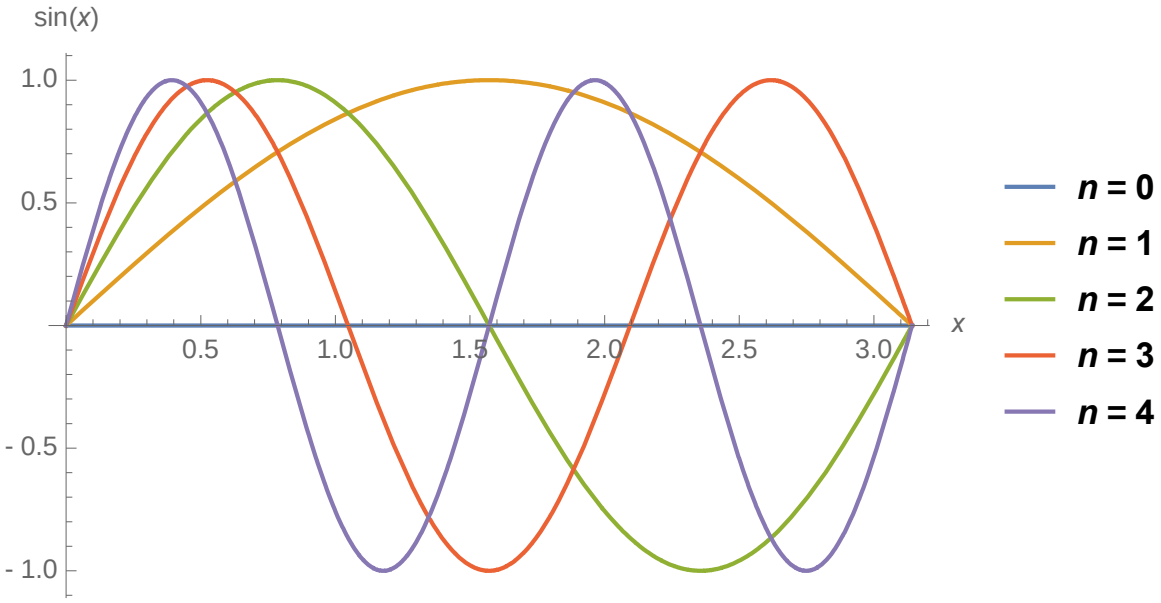

Fig. 3 First five eigenfunctions for $X_n(x)$

Returning to the solution, one can now state that the general solution of the initial problem is a superposition of particular solutions (18), i.e:

$$u(x,t) = \sum_{n=1}^{\infty} A_n sin\left(\frac{\pi n}{R}x\right) exp(-D\left(\frac{\pi n}{R}\right)^2 t), \qquad (19)$$

Values of A_n can be determined using the initial condition (10) and transforming the function f(x) to Fourier series (Gurevich, 2008). As a corollary, the general solution of the initial value problem of one-dimensional diffusion equation (9) with initial conditions (10) and boundary condition (11) is as follows:

$$u(x,t) = \sum_{n=1}^{\infty} \left(\frac{2}{R}\int_0^L f(\zeta)\, sin\left(\frac{\pi n}{R}x\right) d\zeta\right) sin\left(\frac{\pi n}{R}x\right) \exp(-D\left(\frac{\pi n}{R}\right)^2 t) \qquad (20)$$

Where ζ is the transform variable of Fourier transformation.

Solution in cylindrical coordinates

Since delivery system, i.e. a fiber, used in this study is assumed to have a cylindrical axial symmetry, it is more convenient to solve the diffusion equation using cylindrical coordinates.

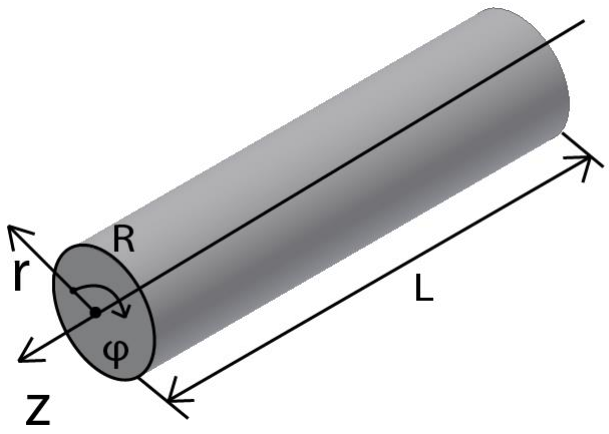

Fig. 4 Schematic representation of a fiber of length L and radius R in cylindrical coordinates.

Considering a long cylinder, in which direction of diffusion is radial only, i.e. concentration is only a function of time t and radius r only, the diffusion equation has the following form (Crank, 1975):

$$\frac{\partial u}{\partial t} = \frac{1}{r}\frac{\partial}{\partial r}\left(rD\frac{\partial u}{\partial r}\right)$$

If the inner and outer radii of the cylinder are 0 and R respectively and the diffusion coefficient D is a constant, i.e. independent on concentration, then the diffusion equation becomes:

$$\frac{\partial \mathrm{u}}{\partial \mathrm{t}} = \mathrm{D}\frac{1}{\mathrm{r}}\frac{\partial}{\partial \mathrm{r}}\mathrm{r}\frac{\partial \mathrm{u}}{\partial \mathrm{r}}, \quad 0 \le \mathrm{r} \le \mathrm{R} \tag{21}$$

The most general initial and boundary conditions for the radial diffusion are (Caretto, 2016):

$$u(r,0) = u_0(r);\ \left.\frac{\partial u}{\partial r}\right|_{r=0,t=0};\ u(R,t) = u_R(t) \tag{22}$$

The following solution steps are based mostly on solution given by Crank (1975) and Caretto (2016). At first we consider the case when u_R is a constant. The first steps of the solution process are similar to the solution in Cartesian coordinates, i.e. method of separation of variables. After splitting function u(r, t) into two functions, we obtain:

$$\mathrm{u}(\mathrm{r},\mathrm{t}) = \mathrm{v}(\mathrm{r},\mathrm{t}) + \mathrm{u_R} \tag{23}$$

Next, the same way as we did in Cartesian coordinates, we divide function v(r, t) into two functions T(t), i.e. function dependent only on time, t, and P(r), i.e. dependent only on the radial coordinate, r, only. We obtain the following:

$$\mathrm{v}(\mathrm{r},\mathrm{t}) = \mathrm{P}(\mathrm{r})\mathrm{T}(\mathrm{t}) \tag{24}$$

After substitution of the equation (24) for u in equation (21) and dividing the obtained equation by the product of DP(r)T(t), the equation (21) becomes:

$$\frac{1}{D}\frac{1}{T(t)}\frac{\partial T(t)}{\partial t} = \frac{1}{P(r)}\frac{1}{r}\frac{\partial}{\partial r}r\frac{\partial P(r)}{\partial r} = -\lambda^2$$

Since the left-hand and right-hand sides of the equation depend only on time, t, and radius, r, respectively, the only case in which equation is correct is if both sides are equal

a constant. For more convenience, the constant is equal to $-\lambda^2$. This leads us to two ordinary differential equations.

The general solution for the first equation is:

$$\mathrm{T(t)} = \mathrm{Aexp}[-\lambda^2 Dt]$$

The second equation can be rewritten the following way:

$$\frac{\partial}{\partial \mathrm{r}} \mathrm{r} \frac{\partial \mathrm{P(r)}}{\partial \mathrm{r}} + \lambda^2 \mathrm{rP(r)} = 0 \qquad (25)$$

which is Bessel's equation of zeroth order. Its general solution is $\mathrm{P(r)=BJ_0}(\lambda r) + \mathrm{CY_0}(\lambda r)$, where $\mathrm{J_0}$ and $\mathrm{C_0}$ are Bessel functions of first and second kind with zero order. The chosen boundary conditions (22) are satisfied by:

$$\mathrm{v(r,t)} = \sum_{\mathrm{m=1}}^{\infty} \mathrm{C_m J_0}(\lambda_\mathrm{m} \mathrm{r}) exp[-\lambda^2{}_\mathrm{m} \mathrm{Dt}] \quad \lambda_\mathrm{m} \mathrm{R} = \mathrm{D_{m0}} \qquad (26)$$

on the condition that $\lambda_m s$ are roots of

$$\mathrm{J_0(D_{mn})} = 0 \quad \text{for} \quad \mathrm{m} = 1, .. \infty \qquad (27)$$

where $\mathrm{D_{mn}}$ denotes the $\mathrm{m^{th}}$ point where $\mathrm{J_n}$ is zero.

L.S. Caretto (2016) emphasizes, in rectangular coordinates, we had to solve equation:

$$\sin\left(\sqrt{\lambda} x\right) = 0$$

(as an interim step for eq. (16)), which was not difficult task as it is known that $\sin(n\pi) = 0$ if n is an integer. On the other hand, it is much more complicated for Bessel function to solve the equation $J_0(\lambda R) = 0$. Nevertheless, zeros of $\mathrm{J_n}$, i.e. the points at which $\mathrm{J_0} = 0$, can be determined. The first five roots of Bessel function, $\mathrm{J_0}$, are presented in Fig. 5, more roots are tabulated in tables of Bessel functions.

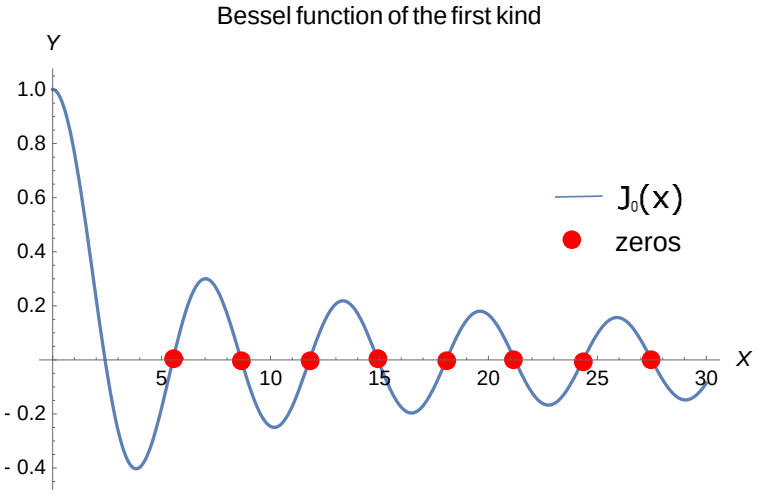

The first five roots of Bessel function, $J_0 m(x)$

m	J_0
1	2.405
2	5.520
3	8.654
4	11.792
5	14.931

Fig. 5 Bessel function of the first kind with zero order and its first five roots

In equation (26) the values can be determined by multiplying both sides of the equation by $J_0(\lambda_m r)$ and integrating from 0 to R. Finally, after some algebra, the solution for u(r,t) satisfying constant initial conditions (22) is:

$$u(r,t) = \sum_{m=1}^{\infty} \frac{2(U_0 - u_R)}{D_{m_0} J_1(D_{m_0})} exp[-D_{m_0}^2 \frac{Dt}{R^2}] J_0(D_{m_0} \frac{r}{R}) + u_R \qquad (28)$$

where J_1 is Bessel function of first kind with first order.

L.S. Caretto (2016) also suggests rearrangement of the equation (28) to achieve a dimensionless form:

$$\frac{u(r,t) - u_R}{U_0 - u_R} = \sum_{m=1}^{\infty} \frac{2}{D_{m_0} J_1(D_{m_0})} exp[-D_{m_0}^2 \frac{Dt}{R^2}] J_0(D_{m_0} \frac{r}{R}) \qquad (29)$$

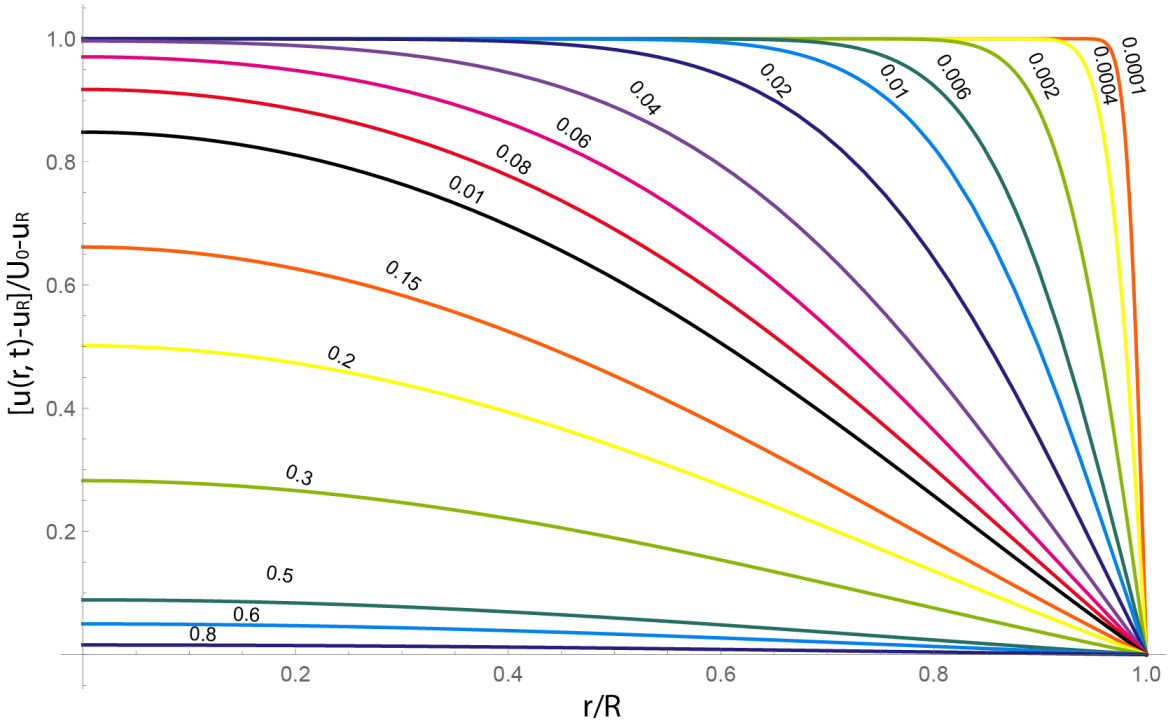

Fig. 6 Solutions for 1D radial diffusion (see Eq. 28) for different values of dimensionless parameter Dt/R^2

Numerical solutions

Presented analytical solutions, namely (20) and (28) are in the form of infinite series. Unfortunately, with respect to the problem considered in this thesis, i.e., diffusion-controlled systems with time, position and concentration dependent diffusion or basically delivery systems with more complex shapes, generally no analytical solution for the diffusion equation exists (Siepmann, Siegel and Rathbone, 2012). On the other hand, the solution of the diffusion equation which more precisely model experimental and practical situations is available using methods of numerical analysis. Nowadays, the advent of the high speed digital processors, allows to get numerical solutions simply using a personal computer. The basic idea of numerical solutions is based on certain approximations, i.e. replacing derivatives by finite differences calculated using time or space grid, however a problem of an error caused by discretization appears (Crank, 1975; Siepmann, Siegel and Rathbone, 2012).

In this study, there was an attempt to determine the diffusivity, *D*, of alaptide through the PCL matrix using a numerical solution. Generally, knowing the diffusivity, one is able to make a quantitative predictions of drug release kinetics within specific matrices, which in turn allows to significantly reduce the number of necessary experiments and to accelerate the fabrication of a drug-delivery product (Siepmann, Siegel and Rathbone, 2012).

Considering the obtained solution for radial diffusion (29), the first approximation can be performed by expansion of Bessel function, J_0, using Maclaurin series as follows:

$$J_0(x) = \sum_{k=0}^{\infty} \frac{(-x^2/4)^k}{(k!)^2}$$

We also assume, that u_R is negligible in this case. Next, to obtain the cumulative amount of alaptide, Q [-], released at time *t*, both sides of the equation (29) should be integrated with respect to space variable, *r*. It was determined empirically, that the number of iterations, k, could be reduced up to 30, otherwise the solution is not stable for higher values of k. Accordingly, the relation (29) yields:

$$\int_0^R \frac{u(r,t)}{U_0} dr = \frac{2}{D_{m_0} J_1(D_{m_0})} exp[-D_{m_0}^2 \frac{Dt}{R^2}] \sum_{k=0}^{30} \frac{1}{(k!)^2} \int_0^R \left(-\frac{1}{4}\left(\frac{D_{m_0} r}{R}\right)^2\right)^k dr$$

Thus, resulting in the identity:

$$\int_0^R \frac{u(r,t)}{U_0} dr = Q = \frac{2}{D_{m_0} J_1(D_{m_0})} exp[-D_{m_0}^2 \frac{Dt}{R^2}] \sum_{k=0}^{30} \frac{{D_{m_0}}^{2k} (-r)^{2k+1}}{4^k (k!)^2 (2k+1)} dr \qquad (30)$$

The relation of between *Q* and *r/R* in dependence on different values of dimensionless parameter Dt/R^2 is depicted in Fig. 7. The values of Dt/R^2 are the same as used in Fig. 6.

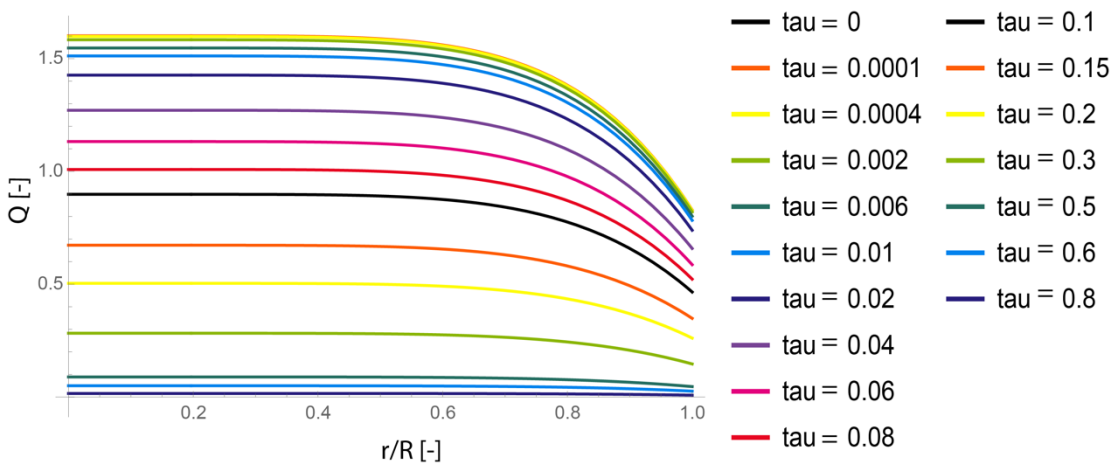

Fig. 7 The relation between the quantity of alaptide released at time t and the space variable r

Nevertheless, the problem is even more complicated by the fact, that we consider diffusivity of a drug on the boundary of two phases, i.e. release medium and the matrix. In this case, a boundary layer mass transfer coefficient, k_c, should be included in the relation (Siepmann, Siegel and Rathbone, 2012). Thus, further steps in determination of diffusivity of alaptide through the polymer matrix will be provided in future study, in particular in the scope of dissertation thesis.

1.3 Diffusion-controlled drug delivery systems

1.3.1 Basic description of the concept

There is constant evolution of the methods of drug delivery. Nowadays, with the increasing recognition of advantages of sustained- and controlled-release drug delivery systems (DDS), there has been growing interest focused on their investigating and developing. As was mentioned in introduction, the main idea of controlled DDS is to achieve a drug release in a controlled manner, i.e. at a predetermined rate and for a sustained period of time. Moreover, drug concentration level should stay within a range between the minimal level, i.e. effective, and the maximal level, i.e. toxic (see Fig. 8).

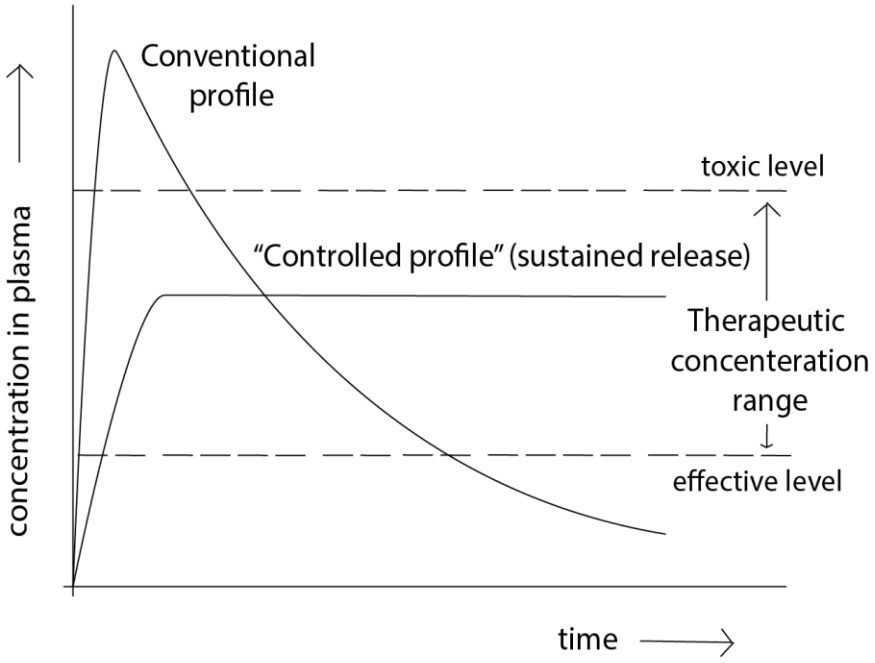

Fig. 8 Comparison of two typical plasma concentration curves for a conventional rapidly releasing dosage and an optimized zero-order controlled release of a drug (reproduced from (Rossi, Perale and Masi, 2016)*)*

The mechanisms involved in controlled-release systems are sophisticated and may vary within the particular site of application (oral, ocular, parenteral, sublingual). Actually, several different mechanisms including diffusion, erosion, partitioning, dissolution, osmosis, swelling, and targeting, may operate at the same moment or at different stages of a delivery process. In this chapter diffusion-controlled systems will be discussed.

An "engine" of diffusion-controlled DDS is concentration gradient occurring between inner and outer space of the device (Rossi, Perale and Masi, 2016). Diffusion-controlled

drug delivery systems are traditionally either matrix-based (*monolithic* system) or *reservoir*-type systems. In matrix-based systems, drug is relatively homogeneously distributed in a continuous matrix composed of a polymer, where water permeation leads to either swelling or osmotically controlled systems. Since the matrix is composed of both the polymer and drug molecules, the swelling effect is seen as a uniform volume expansion of the bulk polymeric material, causing the opening of pores throughout the matrix structure. In the reservoir systems the drug and the release rate controlling material (typically a polymer) are separated according to a core–shell structure, the drug being located in the center and the release rate controlling material forming a membrane surrounding this drug storage (Siepmann, Siegel and Rathbone, 2012; Holowka and Bhatia, 2014). Reservoir systems are able to obtain precise zero-order delivery profile and release rates can be controlled by used polymer type, however they are difficult to fabricate reliably, it's also complicated to deliver high molecular weight compounds, moreover there is a risk of a rapid intoxication if a tear in the membrane would appear. Whereas, matrix systems are easier to produce (Rossi, Perale and Masi, 2016), they provide delivery of high molecular weight compounds, on the other hand it's impossible to obtain precise zero-order release profile, potential toxicity of degraded polymer must be considered, and release kinetics are usually difficult to control (Siepmann, Siegel and Rathbone, 2012; Niraj *et al.*, 2013).

Matrix-type system usually performs an initial burst of release from the surface. Then release rate decreases as drug that is deeper inside the monolith must diffuse to the surface, as the diffusion path length increases, the square relation between distance and time plays a great role. This effect is important for planar monoliths, although it becomes even more significant in case of cylinders- or sphere-shaped systems, because with increasing distance from the surface, the amount of drug available decreases (Siepmann, Siegel and Rathbone, 2012).

Obviously, a further classification of these two diffusion-controlled systems is possible (see Fig. 9). Two subtypes of reservoir systems can be distinguished – either a system with a "non- constant activity source" or a system with a "constant activity source". In reservoir system with non-constant activity source drug solubility is above drug concentration in the reservoir, hereby drug molecules are not replaced after release throughout membrane, so that the drug concentration at the inner surface of the membrane reduces with passing time.

Whereas in a system with a constant activity source, molecules after release are instantly replaced by overage of non-dissolved drug. Therefore, the drug concentration at the inner surface of membrane does not change until drug overage exists. As soon as drug concentration decreases below solubility, the system is considered non-constant activity source type.

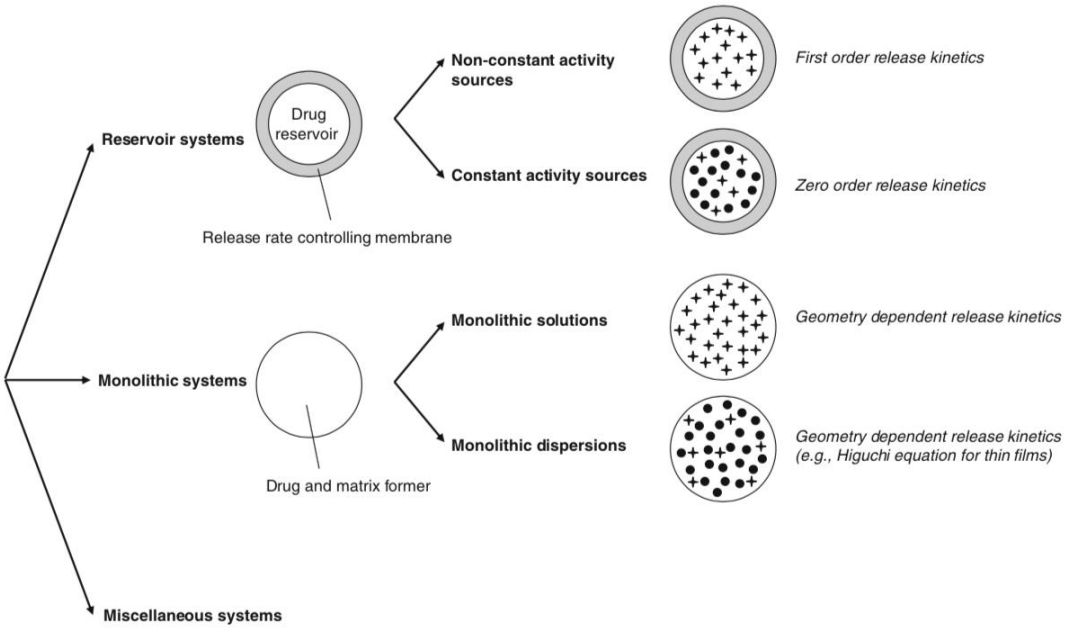

Fig. 9 Scheme for four discussed diffusion-controlled drug delivery systems. Stars represent molecularly dispersed (dissolved) drug molecules. Black circles show non-dissolved drug overage. (Siepmann, Siegel and Rathbone, 2012)

In a like manner, two further subtypes of matrix systems can be recognized according to the initial drug loading:drug solubility ratio. In case of monolithic solutions, drug solubility is above the initial drug loading and the drug is dissolved in the matrix. In monolithic dispersions, drug solubility is below the initial drug loading and the drug is partially dissolved (molecularly dispersed), the residual drug particles can exist across the system in a form of solid drug crystals, amorphous particles, or both. Drug diffusion out of system is possible only after dissolution (Siepmann, Siegel and Rathbone, 2012; Holowka and Bhatia, 2014).

1.3.2 Pharmacokinetics

The release mechanism of a drug release from a matrix devices are strongly dependent on number of factors. Generally, these factors could be divided into polymer-related and

drug-related. A detailed description of most important factors affecting drug release kinetics could be found in a review article by Varma *et al.* (2004). Obviously, it is always desirable to predict release kinetics on the basis of input parameters (see Fig. 10) to accelerate product development by reducing number of experiments that are necessary to perform. Or instead to determine parameters such as e.g. drug diffusivity from the obtained experimental data. Thus, there is a great demand in a development of mathematical models describing drug release from various delivery devices (Dash *et al.*, 2010). To date, a significant number of approaches towards description of release kinetics was developed, however in the following section only some of the basic models will be listed and then applied for a comparison with the obtained data in the *experimental part* of the study.

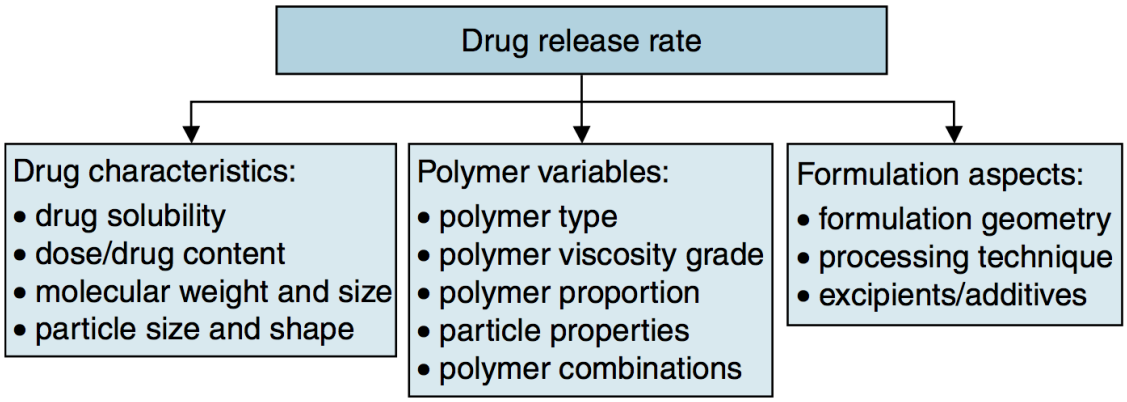

Fig. 10 The main variables of drug release from matrices-based delivery devices (Varma *et al.*, 2004)

According to Dash *et al.* (2010), among different mathematical methods which describe release kinetics, one can distinguish three main categories:

- Statistical methods
- Model-dependent methods
- Model-independent methods

Let us now consider model-dependent methods, in particular *first-order*, *zero-order*, *Korsmeyer-Peppas* and *Higuchi* equations.

Zero-order model

This model can be used to describe the dissolution and release of a low-soluble drug from matrix-based systems or osmotic systems. The zero-order model mostly describes the

most desirable release behavior, i.e. when the release of the drug is independent of drug concentration. The basic relation is expressed as follows:

$$C_t = C_0 + K_0 t \quad (31)$$

Where C_t is the amount of the drug that was dissolved at time t, C_0 is the initial amount of the drug in the release medium (for most cases $C_0 = 0$), K_0 is the zero-order rate constant.

First-order model

The first-order model is usually used to describe the dissolution and release of a water-soluble drug from porous matrices. The rate of a release which follows first-order release is assumed to be proportional to amount of the drug remaining and can be expressed by the following equation:

$$\ln C_t = \ln C_0 + Kt \quad (32)$$

Where C_0 is the initial amount of the drug; C_t is the amount of drug remaining to be released at time t; K is a rate constant expressed in units of time^{-1} (Dash *et al.*, 2010)..

The Higuchi equation

The famous equation to describe drug release from planar diffusion controlled delivery systems was developed by Takeru Higuchi in 1961, which was then expanded for homogeneous matrices with different geometries (Higuchi, 1963; Siepmann, Siegel and Rathbone, 2012). The model is based on a few basic assumptions, which can be summarized as follows:

- the initial drug concentration within the matrix is much higher than drug solubility
- drug particles are significantly smaller than the thickness of the matrix
- swelling and dissolution of the matrix are negligible
- diffusion is one-dimensional only
- the diffusion coefficient of the drug is constant
- the perfect sink conditions are maintained throughout the release process
- the drug is initially homogeneously distributed within the matrix (Dash *et al.*, 2010; Siepmann and Siepmann, 2012)

Accordingly, the Higuchi model can be expressed by the following equation:

$$f_t = Q = A\sqrt{D(2C - C_s)C_s t} \quad (33)$$

Where Q is the amount of drug released in time t per unit area A; C is the initial concentration of a drug, C_s is the solubility of the drug in the matrix media and D is the diffusion coefficient of the drug in the matrix. The Higuchi equation is also frequently used in the simplified form (also known as the simplified Higuchi model), which can be expressed as follows:

$$f_t = Q = K_H t^{0.5} \quad (34)$$

Where K_H is the Higuchi release constant (Dash *et al.*, 2010).

It is important to mention, as emphasises (Siepmann, 2008), the equation (33) is frequently misunderstood and is used for the DDS which do not fulfil the model assumptions listed above. Additionally, even though the cumulative amount of drug released might be proportional to the square root of time, it does not mean that the investigated release involves the same mechanisms as the in the ointment studied by Higuchi. Indeed, different other physicochemical processes might change the release kinetics towards square root of time dependence.

However, the equation (33), as well as its simplified form, can only be used for planar systems. Generally, it is not possible to derive such simple forms for spherical and cylindrical geometries. Thus, the following implicit equation can be used for expressing the fractional release of a drug from the cylindrical carrier:

$$\frac{M_t}{M_\infty} + \left(1 - \frac{M_t}{M_\infty}\right)\ln\left[1 - \frac{M_t}{M_\infty}\right] = \frac{4D}{R^2} \cdot \frac{C_S}{C_{ini}} \cdot t \quad (35)$$

Where, where M_t is the release amount of drug in time t, M_∞ is the equilibrium amount of the drug (or overall amount of drug present), R is the radius of the cylinder, C_{ini} is the initial drug concentration in the matrix (Siepmann, 2012). Nevertheless, in this study it is appropriate to use the simplified form of the equation (33) as the release of the drug is can be also considered as the release from thin nanofibrous layers, not individual fibers.

The Korsmeyer-Peppas model (power law)

Another frequently used simple semi-empirical model to describe the general solute release kinetics of controlled release form non-swellable polymeric devices is the Korsmeyer-Peppas model, also known as *power law*, which is expressed using the following equation (Ritger and Peppas, 1987):

$$\frac{M_t}{M_\infty} = \mathrm{kt}^n \qquad (36)$$

Where k is the constant incorporating structural and geometrical parameters of the DDS, n is the release exponent which indicate the release mechanism of the drug.

Tab. 1 Suggested drug release mechanisms for corresponding values of release exponent n for different geometries (*Ritger and Peppas, 1987).*

Value of exponent, n		**Drug release mechanism**
Thin film	Cylinder	
0.5	0.45	Fickian diffusion
0.5 < n <0.1	0.45< n <0.89	Anomalous transport
1.0	0.89	Polymer swelling

In Tab. 1, anomalous transport stands for case when different physicochemical phenomena overlap, mainly involving drug diffusion and polymer swelling. The n > 1 indicates the erosion-controlled release (Holowka and Bhatia, 2014).

2 Experimental part

2.1 Materials and methods

2.1.1 Polycaprolactone

Poly-ε-caprolactone (PCL) is linear hydrophobic aliphatic semi-crystalline polymer synthesized by ring-opening polymerization of ε-caprolacton (Yarin, Pourdeyhimi and Ramakrishna, 2014). Nowadays, with increasing development of electrospinning technique, PCL has been getting great attention in healthcare field and tissue engineering due to its desirable characteristics (Ravi Kumar, 2016), such as biodegradability, biocompatibility, low cost of raw materials, high solubility in organic solvents, e.g. THF, chloroform, methylene chloride, benzene, toluene, cyclohexanone, even at room temperatures (Chasin and Langer, 1990; Qin, 2015) , and finally, high tensile modulus, i.e. 400 MPa according to (Thomas *et al.*, 2006), which increases mechanical properties of scaffolds and delivery devices. Moreover, it is known, that hydrophobic polymers as drug delivery devices, can sustain and control drug release for longer periods (Siepmann, Siegel and Rathbone, 2012), that is desired for delivery systems described in chapter 1.3.1. Finally, a capacity to successfully form stable blends with other polymers, motivated great number of studies, as well (Chasin and Langer, 1990). On the other hand, low glass transition and melting temperatures, i.e. –60 °C and 55–60 °C, respectively, could be considered as one of the main disadvantages. For instance, in case of sterilization, low melting temperature does not allow PCL to be proceeded as conventional thermoplastic polymers, e.g. by autoclaving (Horakova *et al.*, 2017). Nevertheless, the melting temperatures range is strongly dependent on crystallinity of PCL, which in turn can be driven by molecular weight and to certain extent on process of fabrication (Ravi Kumar, 2016).

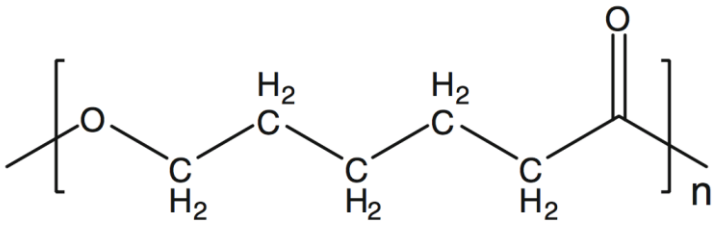

Fig. 11 Structure of PCL, n denotes number of caprolactone units (Siepmann, Siegel and Rathbone, 2012).

2.1.2 Alaptide

Alaptide (8(S)-methyl- 6,9-diazaspiro[4,5]dekan-7,10-dione), spirocyclic synthetic dipeptide, is an original Czech compound, which was firstly discovered in the 1980s by Šturc and Kasafírek in Prague. It was synthesized as an analogue of melanocyte-stimulating hormone release-inhibiting factor (MIF). From the series of other spirocyclic derivatives alaptide was chosen as the most advantageous MIF analogue from the point of enzymatic stability and due to its pharmacodynamical profile (Jampilek *et al.*, 2014).

Though alaptide can be classified as nootropic, e.g. it was experimentally found to have an effect alaptide on behavior and learning abilities of rats and mice, but in this study alaptide was used mainly for its results in dermatological experiments: number of tests showed an ability of alaptide to positively influence epidermal regeneration. In vivo experiments were performed on domestic pigs, rats and mice, proved that alaptide accelerate skin regeneration and curing of experimental skin injuries. Moreover, very low acute toxicity was observed in rats and mice, i.e. 1g/1 kg dose caused only 20% mortality of female rats (Jampilek *et al.*, 2014). Alaptide is now successfully used as veterinary ointment ALAPTID® (Bioveta, Czech Republic) for treatment of warm-blooded animals in order to cure local injuries as burns, frost-bites, bedsores, etc. (Julínek et al., 2010).

Alaptide is a white crystalline compound with melting point 308–312 °C. It is sparkly soluble – particularly, its solubility in water is 0.1104 g/100 mL, in ethanol 0.1011 g/100 mL, in the mixture water/ethanol (1:1) 0.3601 g/100 mL and in hexane 0.0024 g/100 mL (Dragicevic and Maibach, 2017).

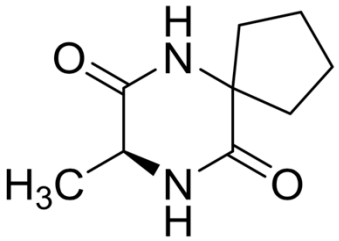

Fig. 12 Structure of (S)-Alaptide molecule (Dragicevic and Maibach, 2017).

2.1.3 Preparation of PCL nanofibrous mats

Poly-ε-caprolactone (Mw 43 000), purchased from Sigma-Aldrich GmbH, was dissolved in a chloroform/ethanol solution system (9:1 by weight) with the polymer concentration

of 16 wt. %. Then 75 mg of sodium lauryl sulphate (SLS) was added as a stabilizer. The final weight of the polymer solution was 100 g. The solution was subsequently stirred and then electrospun with a NANOSPIDER^{TM} equipment to make control nanofibrous layer without alaptide. The same procedure was followed to form modified materials with addition of alaptide of three different concentrations, namely 0.1 wt. %, 1 wt. % and 2.5 wt. %. Accordingly, after the evaporation of the solvent, the actual alaptide loading was 0.625, 6.25 and 15.625 wt.% respectively. However, for convenience in the following text by the term "drug loading" will be meant the concentration in the original polymer solution (suspension), i.e. 0.1, 1 and 2.5 wt. %.

2.1.4 Morphological analysis

In order to investigate the morphology of obtained electrospun mats, small fibrous samples (about 0.5 cm x 0.5 cm) were cut out the mats, coated with 14 nm of gold and then analyzed using a scanning electron microscope TESCAN Vega 3SB (Czech Republic). Both sides of the mats were analyzed. The fiber diameters were subsequently determined, using an image analyzer ImageJ (National Institutes of Health, MD, USA). The measurement was performed in two steps. At first, the scale bar on a selected SEM image was converted to a pixel scale by drawing a line over the scale bar. Then, individual fibers were measured manually. The final fiber diameter of fibrous mats was evaluated as mean values of 200 measurements in various spots on four different SEM images, i.e. 50x measurements on each image with magnification 5000x.

2.1.5 Preparation of PBS with Sodium azide

A release profile of a drug significantly depends on the chosen release medium. It is known from literature, that Phosphate-buffered saline (PBS) with a pH of 7.4 is used for *in vitro* investigating of the release kinetics of a drug in majority of studies. To prepare 2-liter solution of PBS with sodium azide the reagents listed in the Tab. were dissolved in 1600 mL of distilled water. The reagents were added in the same order as mentioned in the Table. Then, obtained solution was kept mixing for a while. After that, pH was adjusted to 7.4 with hydrochloric acid and then distilled water was added to a total volume of 2 L. Finally, 0.4 g of sodium azide (NaN_3) was added to the solution in order to prevent biological infestation and growth. The final solution was dispensed into aliquots (0.5 L each) and sterilized by autoclaving.

Tab. 2 List of reagents and its amount used for preparation of PBS (pH 7.4) solution

Reagent name	Chemical formula	Amount [g]
NaCl Sodium chloride	NaCl	16
KCL Potassium chloride	KCL	0.4
Sodium phosphate dibasic dihydrate	Na_2HPO_4	7.26
Monopotassium phosphate	KH_2PO_4	0.48

2.1.6 *In Vitro* release test of alaptide

For investigation of alaptide release, small nanofibrous samples with average weight of 50±0.9 mg were cut from the nanofibrous layers of each material (with 0, 0.1, 1 and 2.5 wt.% alaptide), and then divided into three sets (three samples in each set) according to the sterilization method. The first set of samples (set I) was sterilized by rinsing in 5 mL of 70% ethanol for 30 minutes. The second set (set II) and the third set (set III) were sterilized by ethylene oxide. The fourth set of samples (set IV) was kept as non-sterilized. The samples from the sets II and IV were first rinsed in 5 mL of PBS (pH 7.4) solution. Next, these samples were carried out the rinsing tube and immersed into a 5 mL of fresh PBS (pH 7.4) solution. The samples from the set III were immersed into PBS solution without preliminary rinsing. Afterwards, all the samples (except set I) were incubated in CO_2 incubator at 37± 1 °C. At predetermined time intervals (1 h, 5 h, 24 h, 7 days and 14 days) some small aliquots of 1 mL were taken out from the tube and replaced with a fresh PBS solution to maintain sink condition. All the collected aliquots were cooled until the end of experiment. After 14 days of the experiment, the obtained aliquots were analyzed using gel permeation chromatography (GPC). The cumulative amount of released alaptide was calculated using the following equation:

$$U = C_{s(t)} \cdot V_{tube} + (V_s \cdot \sum C_{s(t-1)}) \quad (37)$$

Where $C_{s(t)}$ [mg/L] is a concentration of alaptide in aliquot sample at time *t*, V_{tube} [L] is the overall volume of the tube with the release medium (5 mL), V_s [L] is the volume of an aliquot (1 mL). Then the cumulative amount of alaptide released was plotted as a function of time.

Three different factors influencing the drug release were studied within the experiment, i.e.:

- effect of initial drug loading,
- effect of used sterilization technique
- effect of preliminary rinsing in PBS.

2.1.7 GPC analysis

Determination of alaptide concentration in each collected aliquot, as well as dissolved fibrous samples, was carried out using gel permeation chromatography (GPC). The HPLC system used was a Dionex Ultimate 3000 with a LPG-3400SD quaternary gradient pump, a SR-3000 solvent rack, a WPS-3000TSC autosampler, a TCC-3000SD column compartment and a DAD-3000 detector. A Phenomenex Kinetex Hilic core-shell column with a length of 150 mm and internal diameter of 4,6 mm was used. The aqueous component (A) of the mobile phase consisted of 5 % acetonitrile in water. The organic component (B) of the mobile phase consisted of pure acetonitrile. A set linear gradient was used. At the start the proportion of B in the mobile phase was 90 %. At 1.5 min begun a one minute lasting gradient from the initial conditions to 60% of B component. This composition of the mobile phase was kept for one minute and then returned in 0.5 minutes to initial conditions. The chromatogram for each sample was recorded for 6.6 min. The flow rate was 1.5 ml/min and the column was kept at 20°C. The injection volume used was 20 µL. The chromatograms were recorded at wavelengths of 200, 205, 210 and 250 nm with a sampling rate of 2 Hz.

The aliquot samples were diluted by pure acetonitrile by pipetting 150 µL of the sample and 1500 µL of acetonitrile into a 2-mL vial and vortexing. The samples were filtered through a 13-mm diameter nylon syringe filter with a pore size of 0.22 µm prior to injection.

Likewise, amount of alaptide released to a DMEM was quantified. The aliquot samples were diluted by 90% acetonitrile by pipetting 150 µL of the sample and 1350 µL of acetonitrile into a 2-mL vial and vortexing. The samples were filtered through a 13-mm diameter nylon syringe filter with a pore size of 0.22 µm prior to injection.

Similar procedure was followed in order to quantify an amount of alaptide trapped in the nanofibrous layers after the 14-day experiment. The nanofibrous samples were dissolved

in 4 mL of chloroform/acetonitrile (1:1) solution and then vortexed. The obtained solution with dissolved fibers was diluted by pipetting 2 mL of the solution and 2 mL of pure methanol and vortexing. Finally, the sample solution was diluted by pipetting 850 µl of the sample solution, 150 µl of distilled water and 3 mL of pure acetonitrile into a 4-mL vial and vortexing. Two milliliters of each sample solution were filtered through a 13-mm diameter nylon syringe with a size of 0.22 µm prior to injection.

2.1.8 Revealing the presence of PBS crystals after drying

On a few samples after drying a slight weigh gain was detected, whereas no weight gain was observed on samples without alaptide. This weight gain could be caused by crystals of PBS, as none of samples was rinsed with distilled water after removing from PBS solution at the end of the 14 days of incubation. Therefore, the following experiment was performed in order to proof the presence of PBS crystals on nanofibrous samples. First of all, six nanofibrous samples (50±0.9 mg each) were cut out from the same PCL layer as mentioned in the main experiment. Then, all the samples were immersed into 5 mL of PBS and were kept incubating at 37ºC for 14 days. Afterwards, each sample was removed from the PBS solution and only three of them were rinsed with distilled water. Each sample (rinsed and non-rinsed) was kept drying at 26 ºC for 48 hours. After 48 hours of drying, all the samples were weighted. Taking into account the mean value of alaptide content which was released for individual samples, the actual weight difference, *WD* [mg], was calculated as follows:

$$\mathrm{WD} = (\mathrm{m}_a - m_b + m_r) \cdot 1000 \qquad (38)$$

Where m_a is the weight of dry sample at the end of the experiment, m_b is the original weight of the sample before the experiment, m_r is the amount of alaptide which was released for the corresponding sample during the 14-days *in vitro* release experiment.

2.1.9 Contact angle measurement

Determination of a contact angle of the electrosppun nanofibrous layers was carried out on See System E equipment (Advex Instruments, LLC), using a sessile drop technique on a See System E (Advex Instruments, LLC), by pipetting a droplet (15 µL) of distilled water on the surface of the layer. Immediately after pipetting the droplet was multiply captured by a camera every 0.1 second. Afterwards, mean values of dynamic contact angle from 5 measurements on different spots of the layer were plotted as a function of time (Fig. 13).

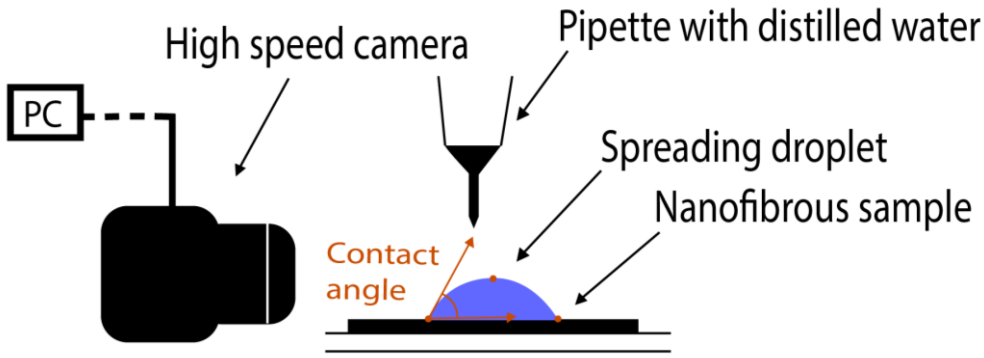

Fig. 13 Experimental setup for measurement of a contact angle. The camera is connected to the personal computer (PC) with analyzing software. The contact angle is then determined on the basis of three red points forming a circle along the droplet surface.

2.1.10 Influence of material extracts on a cell viability.

Small samples with mean weight 50 ± 2 mg, were cut from electrospun nanofibrous layers and put inside 15 mL tubes. Subsequently, all the sample were exposed to sterilization cycle with ethylene oxide (Anprolene). After one-week airing electrospun samples were immersed in 5 mL of (DMEM + 10% fetal bovine serum + 1% mixture of antibiotic – penicillin, streptomycin, amphotericin B +1% glutamine, Biosera). Release of alaptide were investigated in predetermined time intervals, namely 1, 5, 24 hours, 7 and 15 days, similarly as for the experiment with release to PBS solution. After each time interval, a small aliquot of 1 mL was taken out from the tube and frozen for further analyses. Each aliquot was replaced with a 1 mL of fresh DMEM to maintain sink condition. Also, a control sample of pure DMEM was frozen before the experiment. Subsequently, each frozen aliquot was assessed in terms of i*n vitro* using mice fibroblasts 3T3-SA (ATCC). Methods of assessment are defined in norm ČSN EN ISO 10993-5 Biological evaluation of medical devices – Part 5: Tests for in vitro cytotoxicity (2009). The first day of the experiment the cells were placed in a 96-well cell culture plates (passage No. 19) with concentration of 10^4/well. The next day morphology of the cells and its confluence were assessed microscopically. Afterwards, frozen aliquots were defrosted and added to the confluent cells layer (100 µl). The same amount of pure DMEM, which was frosted before the experiment, was added to the control cells. To proof an efficiency of the test, a viability of cells with 0.1% of Triton X-100 was investigated. At the end cells were kept incubation for 24 hours at 37°C. The next day the cells DMEM/extracts were sucked out from the wells and then 110 µl of DMEM with 10% of cck-8 (Dojindo, Inc.) was added.

The prepared plates were then kept incubating for 2.5 hours and subsequently an absorbance of the solutions was measured at wavelength of 450 nm (TECAN). The obtained values for the absorbance of the control cells was considered as 100% of cells viability. The absorbance of the rest of the cells was related to this value, providing percentage of cells viability. Overall count of replicate measurements was 12.

2.1.11 Fitting of the curves to mathematical models

In order to understand the kinetics of alaptide release, the release data of alaptide were fitted in the mathematical models described in the section 1.3.2, namely zero-order, first-order, Higuchi and Korsmeyer-Peppas. The compliance of the fitting was determined by comparing the average values of determination coefficient, R^2. The release constant k was determined from the most relevant fitting model.

2.2 Results

2.2.1 Morphological analysis of electrospun samples

The PCL nanofibrous layers were electrospun from 16% PCL with and without alaptide. Different drug loading led to various morphologies as shown in Fig. 15. Obtained fiber diameter distribution is depicted in box-plot graph below.

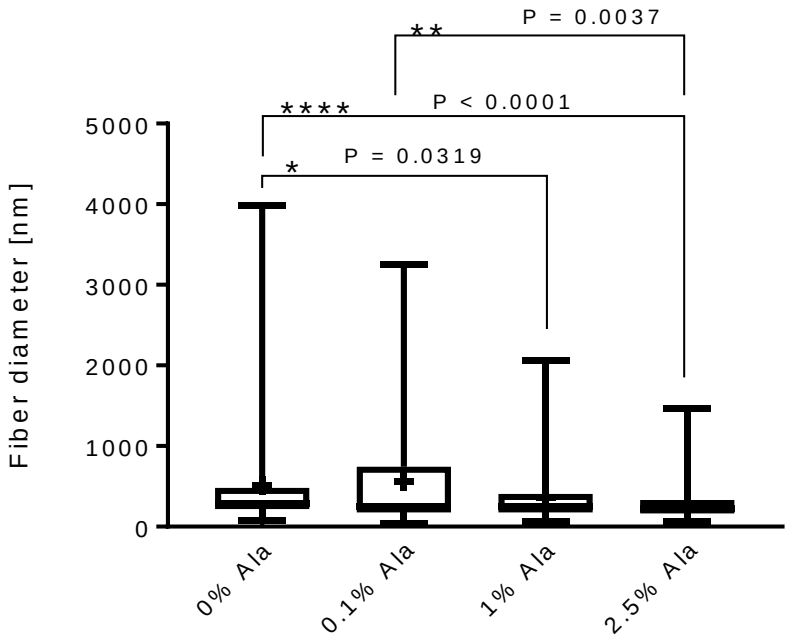

*Fig. 14 Box-plots of fiber diameters distribution for four PCL nanofibrous mats with four different initial loading of alaptide; * denotes statistically significant differences between box-plots*

Mean of fiber diameter was in a range of hundreds of nanometers. Some of the fiber diameters were in a range of microns. The thinnest fibers (308.87 nm, <275; 343> nm) were achieved from solution with the highest loading of alaptide (2.5 wt. %). It is clear from SEM images, that there is a wide range of fiber diameters, however mat with two highest alaptide loadings (1wt.% and 2.5 wt.%) had the narrowest diameter range. Narrowing of fiber diameters range is also illustrated in Tab. 3, which reveals that with increasing of drug loading, decreased the difference between mean and medial values for each sample.

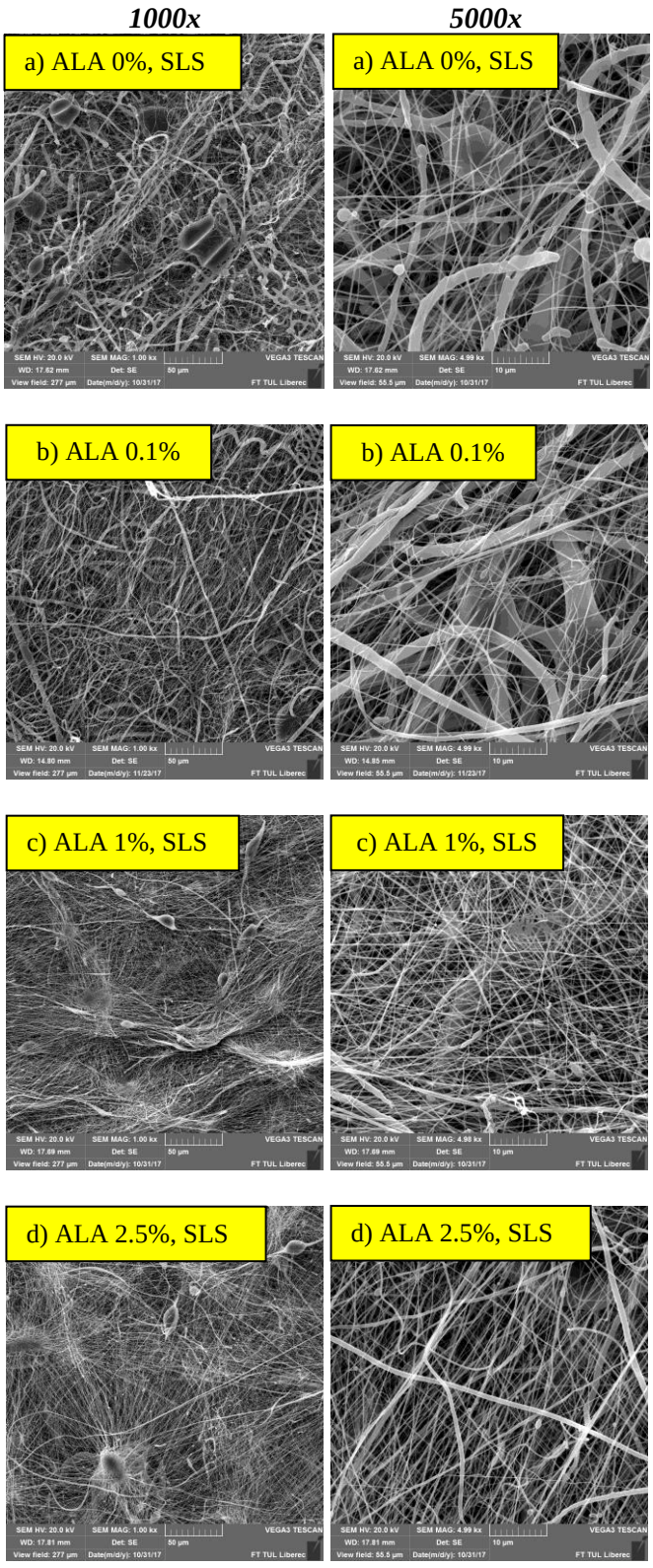

Fig. 15 Scanning electron images of electrospun samples – two images in row with different magnification for each of these samples: (a) non-modified PCL fibers (from chloroform/ethanol 9:1 solution with addition of SLS); (b) PCL fibers (from chloroform/ethanol 9:1 solution) modified with of 0.1 wt. % of alaptide; (c) PCL fibers (from chloroform/ethanol 9:1 solution with addition of SLS) modified with of 1 wt. % of alaptide; (d) PCL fibers (from chloroform/ethanol 9:1 solution with addition of SLS) modified with of 2.5 wt. % of alaptide. The scale is 50 µm on the left and 10 µm on the right.

Moreover, increasing of drug loading led to decrement of number of beads and increment of smoothness of the layers. The layer with 0.1% loading was prepared without adding a stabilizing surfactant (SLS) to the polymer solution. It caused stickiness of the mat and forming of great number of beads (probably alaptide particles) on the surface.

Fig. *14* reveals that increasing of drug content actually changed distributions of fiber diameters. One can see that there is a great statistically significant difference ($P < 0.0001$) between the control sample without alaptide and the sample with the highest used loading, i.e. 2.5 wt.%. Although, there is no statistically significant difference between the control sample and the sample with the lowest drug loading, i.e. 0.1 wt.%. Nevertheless, these two samples (0 wt.% and 0.1 wt.%) had significantly different range of fiber diameters, which can also be partially seen from *Tab. 3*, where standard deviation (SD) and 95% confidence interval (CI) of mean are wider, i.e. <423.5-585.5> vs. <475.3; 656.9>. Despite all the samples had its medians of fiber diameters close to each other, mean values were not consistent.

Tab. 3 Selected values of descriptive statistics of the distribution of fiber diameters

	Ala 0%	**Ala 0.1%**	**Ala 1%**	**Ala 2.5%**
Number of values	200	200	200	200
Median [nm]	295	252	252	226.5
Mean [nm]	504.52	566.12	356	308.87
SEM [nm]	41.09	46.05	21.45	17.32
SD [nm]	581.08	651.22	303.37	245
95% CI [nm]	423.5 - 585.5	475.3 - 656.9	313.7 - 398.3	274.7 – 343

2.2.2 Morphology of samples after the experiment

Investigation of the dried electrospun layers after the 14-days experiment revealed no remarkable changes in the morphology of control samples (see Fig. 16). However, significant changes were observed in case of drug-loaded samples. As depicted in *Fig. 17*, release or washing of the drug from the samples caused increment of smoothness of the layers' surface. At the same time, the drug-loaded samples were also found to be wrinkled. These morphology changes were more visible with increasing in drug loading.

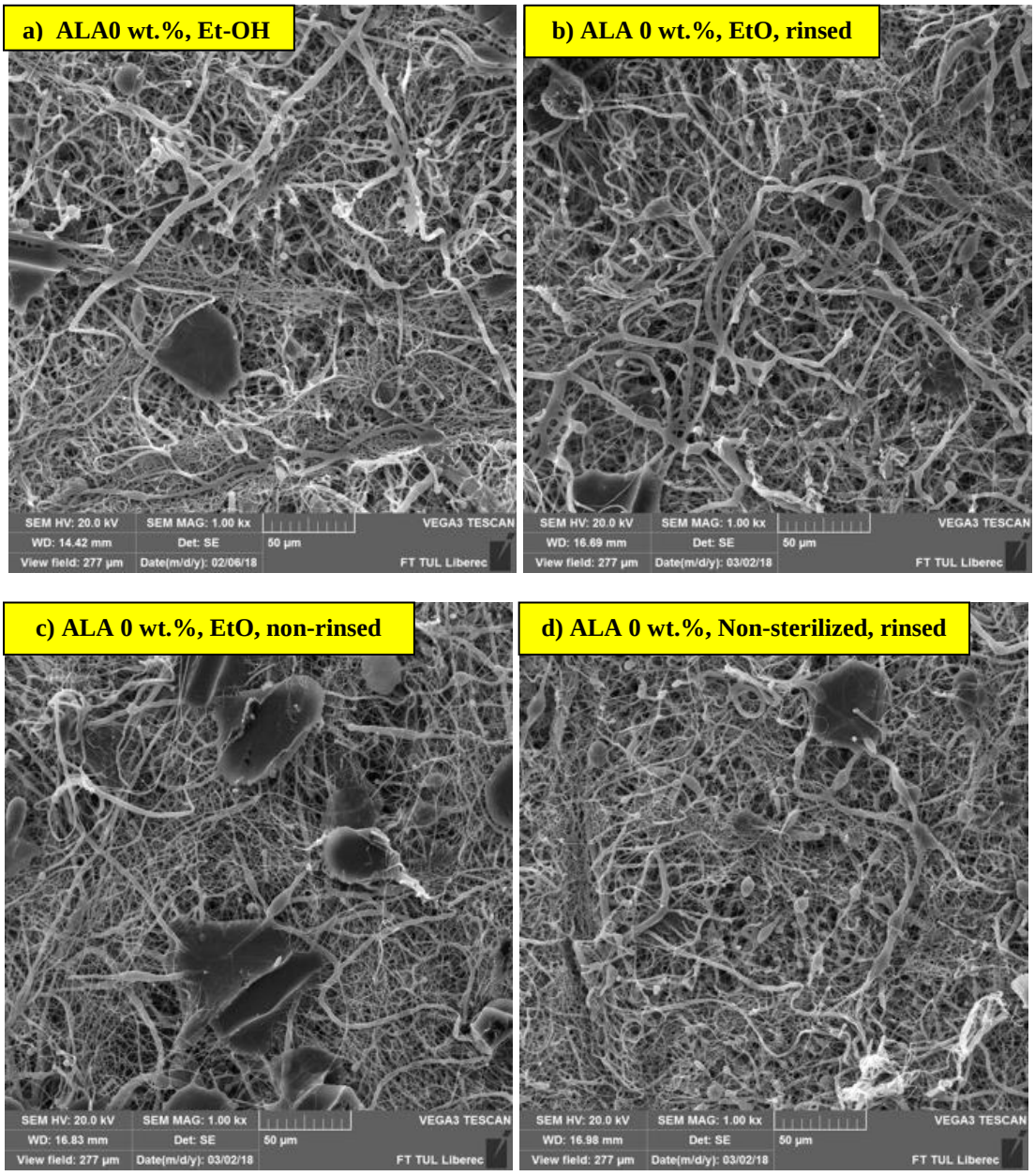

1000x

Fig. 16 Scanning electron images of electrospun control samples without alaptide after 14-day experiment.

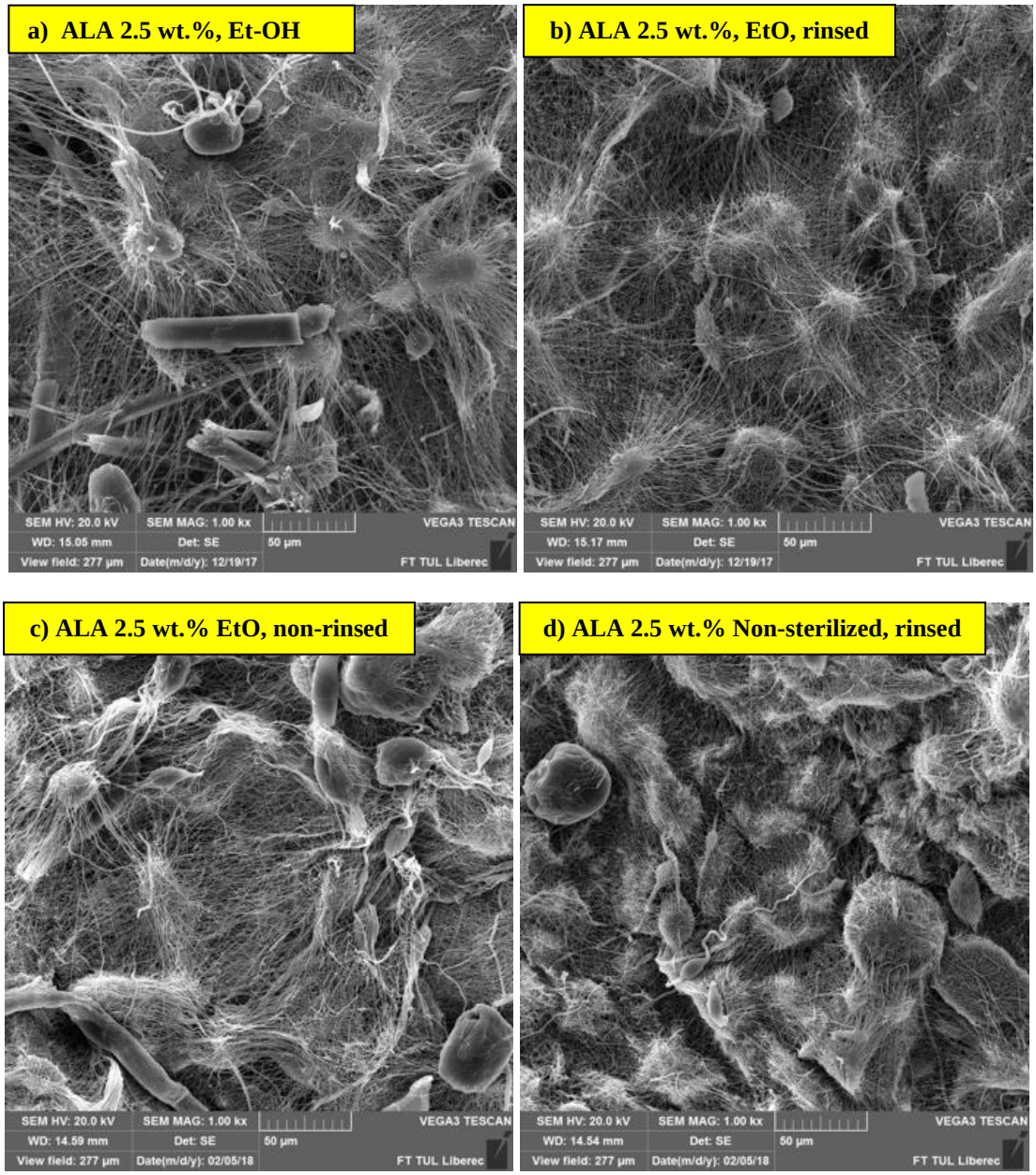

1000x

Fig. 17 Scanning electron images of electrospun samples with 2.5 wt.% loading of alaptide after 14-day experiment.

Moreover, there were observed small particles (~15 µm), which are assumed to be adsorbed crystals of PBS salts. Their quantification is described in the section 2.2.3. No significant difference in morphology between rinsed and non-rinsed samples was observed as well as the difference between non-sterilized samples and samples sterilized with EtO or EtOH.

2.2.3 Results of revealing the presence of PBS crystals after drying

The actual weight difference before and after experiment was calculated for each drug loading using equation (38). It was also expressed as the fraction with respect to the original weight of the samples. The results are presented in Tab. 4

Tab. 4 Real weight difference of dry samples before and after 14-day incubation, taking into account released amount of alaptide evaluated with GPC analysis

Real weight difference concerning the released amount of alaptide (MEAN ± SD, n=3)		
	mg	**%**
Ala 0 wt.%	1.467 ± 0.41	2.933
Ala 0.1 wt.%	3.433 ± 0.78	6.867
Ala 1 wt.%	4.705 ± 0.53	9.411
Ala 2.5 wt.%	4.508 ± 0.25	9.016

2.2.4 Results of contact angle measurement

As the layers with higher loadings of alaptide, i.e. 1 and 2.5 wt.% alaptide turned out to be remarkably more hydrophilic than the two other layers, and the droplet was immediately absorbed by a layer, it was impossible to measure a contact angle statically. Thus, a dynamic approach was used to determine a contact angle as a function of time within 1 second interval. It can be visualized from Fig. 18, that there is a significant standard deviation for a control sample (0 wt.% alaptide) and the sample with the lowest drug loading (0.1 wt.%). This SD was caused by heterogeneity of the layers, in particular by fact that a droplet of distilled water either was stable for approximately 2 minutes or was absorbed within a few seconds. The same reason caused a decreasing character of curves for 0 and 0.1 wt% (see Fig. 19), as in fact, in majority of measurements the droplet was stable and was not absorbed within given period of time, so the function should be constant. Heterogeneous structure also influenced initial angle i.e. a contact angle measured immediately after pipetting a droplet., as it differed at different spots of the layers. Although the slopes of plots for the two higher drug loadings, i.e. 1 and 2.5 wt.%, were almost the same (-49.827 and -48.722 respectively), the initial contact angle is different (86.02 ± 11.70 and 67.16 ± 16.11 respectively).

Fig. 19 depicts relationship between drug loading and an initial contact angle. It is clear from the plot that hydrophilicity of electrospun layers increased almost linearly (R^2=0.895) with the increasing drug loading.

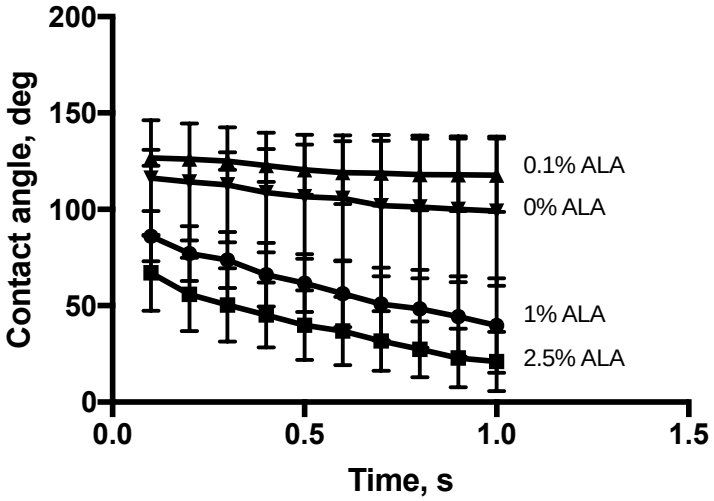

Fig. 18 Measurement of a contact angle of PCL layers as a function of time

.

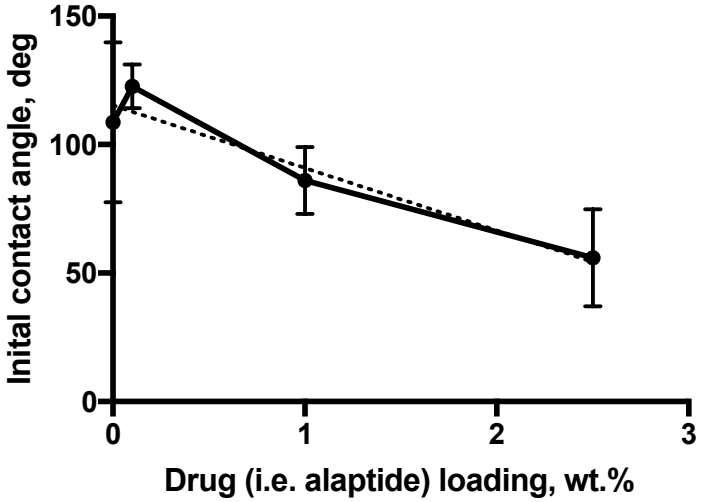

Fig. 19 Initial contact angle (measured immediately after a drop lands on the surface of a sample) decreases with increasing drug loading.

Nevertheless, used method is very sensitive to a number of variables, e.g. height from which droplet was pipetted, angle of pipette, and subsequently on a placement of control points (see red dots in Fig. 13). Moreover, used material is highly contrast, this fact complicated a proper placement of control points, as a border between a material and a droplet was hardly visible. Thus, different types of lighting and overshadowing backgrounds were tested.

Indeed, the obtained values of the contact angle are not absolute values due to heterogeneity of the electrospun layers. Although, these values can be used as indexes for comparison of wettability of the electrospun layers.

2.2.5 *Results of in vitro* tests of alaptide release

The release of alaptide at different initial loadings, namely 0.1 wt. %, 1% wt. % and 2.5 wt. %, was studied in PBS (pH 7.4) solution at 37ºC. Three aspects of release were investigated within the experiment, particularly effect of initial drug loading, effect of sterilization and finally an effect of preliminary rinsing. The cumulative release profiles of alaptide versus time (mean of three samples) are plotted in Fig. 20 for all the concerning all the three aspects.

Effect of initial drug loading

Fig. *20* shows that release kinetics at the lowest loading of alaptide, i.e. 0.1 wt.%, significantly differ from the two higher loadings. An increased drug loading increased release rate of the drug. Almost a complete initial drug loading content, i.e. 78% (SD 1.2, n=3) and 82% (SD 1.7, n=3), had been released within first 24 hours for the non-rinsed sterilized samples at loadings of 1 wt. % and 2.5 wt. respectively % (Fig. 20b, 1c). Within next 312 hours only additional 1.7% (SD 1.06) and 3% (SD 0.65) were released. Whereas for non-rinsed samples at 0.1% drug loading, release sustained over 14 days resulting in 49% (SD 2.57; n=3) of alaptide released at the end of the experiment.

Effect of sterilization

It is clear from Fig. 20, that there is no remarkable difference between release profiles of non-sterilized PCL nanofibrous samples in comparison with sample which were exposed to sterilization by ethylene oxide. As in the case of non-sterilized samples at higher drug loading, namely 0.1 wt.% and 2.5 wt.%, initial burst release is observed. At 1% drug loading, this burst caused 43% (SD 4.1, n=3) and 40% (SD 2.1, n=3) release within first 24 hours for rinsed and non-rinsed sterilized samples respectively.

Effect of preliminary rinsing

According to the results in Fig. 20, the cumulative percentage of released alaptide achieved by non-rinsed samples at the end of the experiment was approximately twice as much in comparison with preliminary rinsed samples. However, GPC analyze of aliquots of PBS solution used for preliminary rinsing, revealed (see Tab. 6), that more than a half of initial drug loading content was washed out before the start of the experiment. In other

word, both non-rinsed and rinsed samples achieved almost complete release of the drug loading combining both washed out and released drug content.

As mentioned above, each sample underwent an initial burst release, Fig. 21 shows release profiles of these two higher drug loadings (with a more pronounced burst effect) within first 24 hours of the experiment.

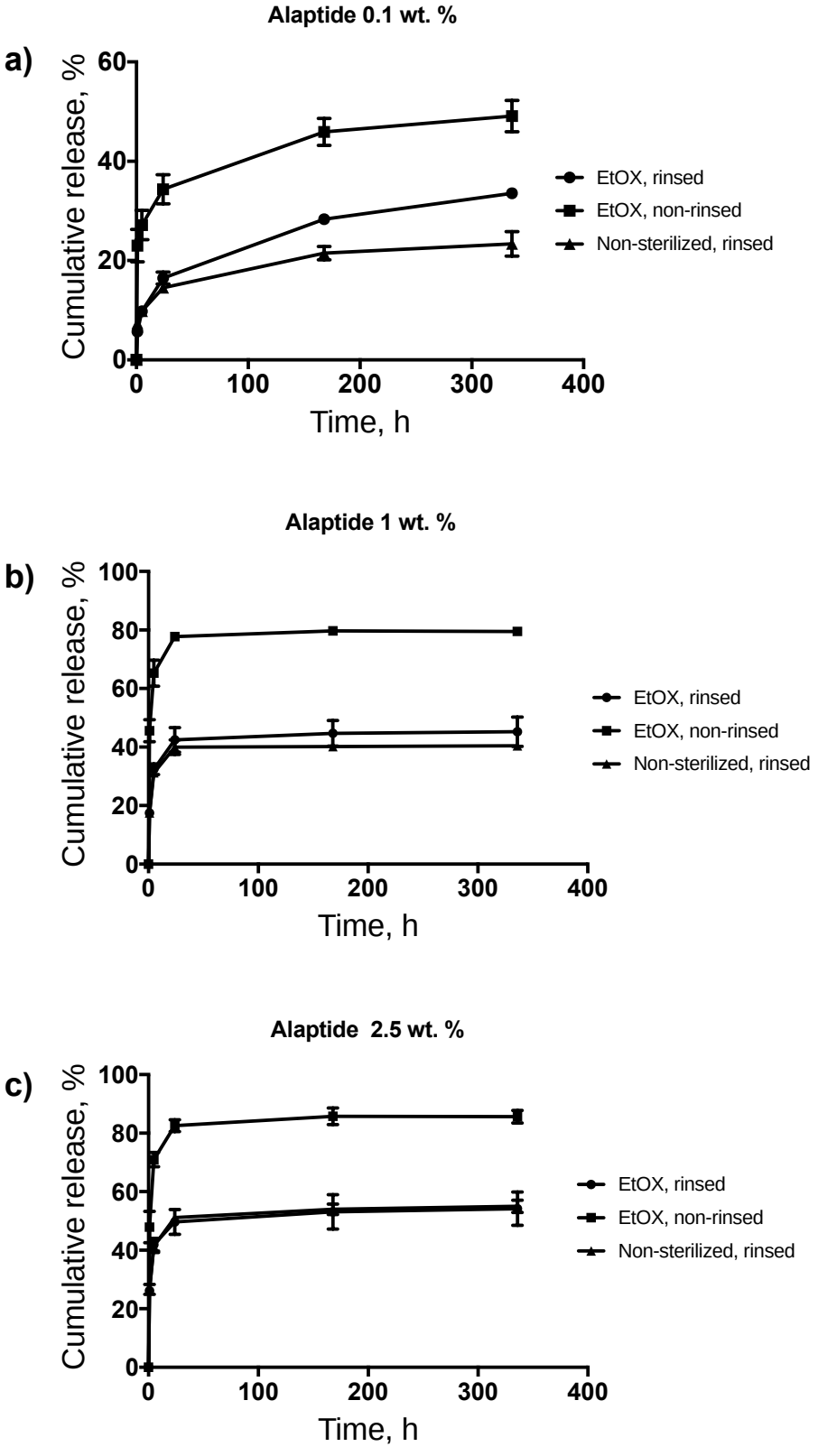

Fig. 20 Cumulative release profiles of Alaptide from electrospun PCL nanofibrous mats. Three different initial Alaptide loading are presented: (a) 0.1 wt.%, (b) 1% wt. %, (c) 2.5 wt. %. Individual curves on each graph represent the method of sterilization of PCL layers. Each point represents mean ± SD, n=3

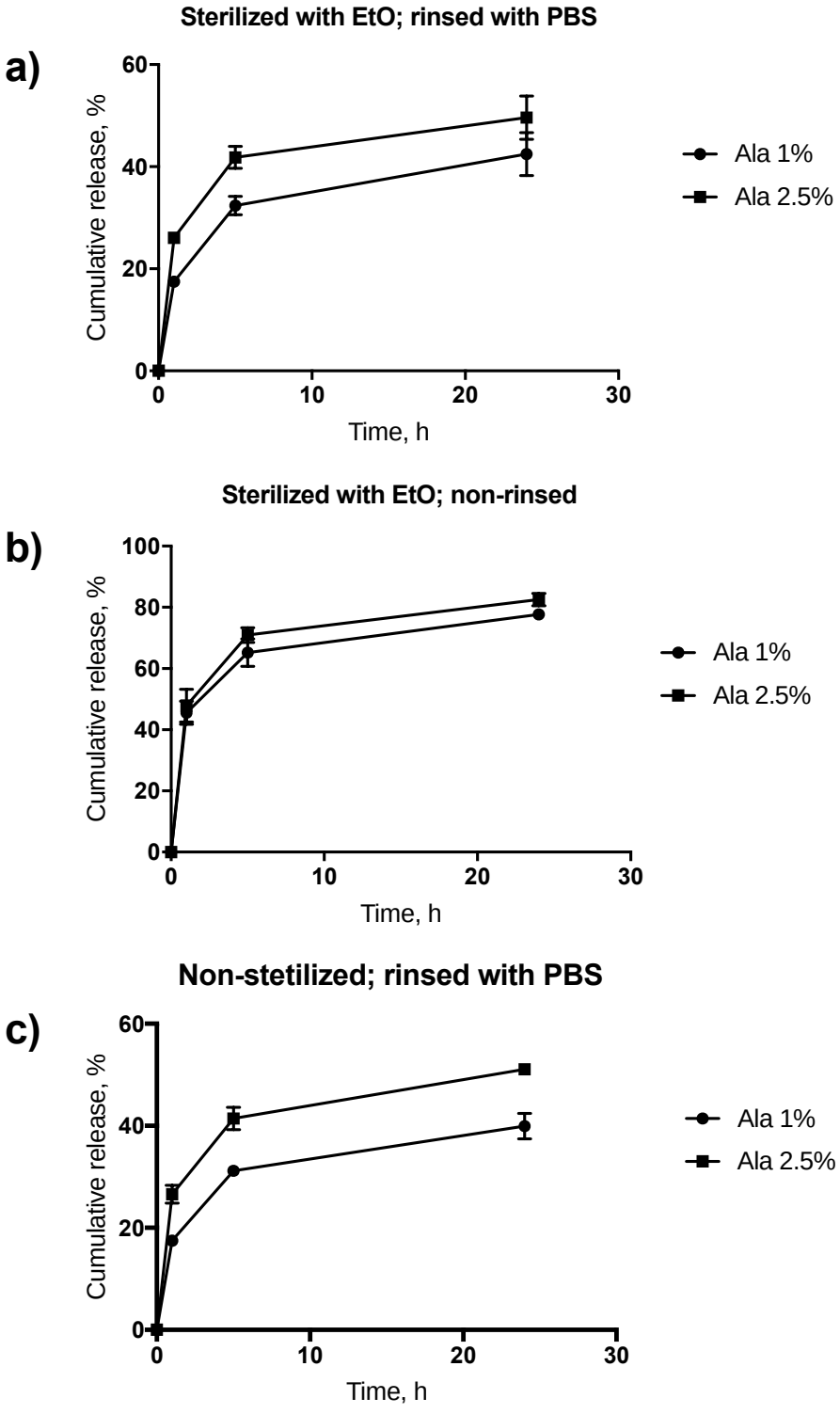

Fig. 21 Comparison of burst release profiles at higher loadings, i.e. 1 and 2.5 wt.%, of alaptide within first 24 hours of the experiment: (a) nanofibrous sample sterilized with ethylene oxide, preliminary rinsed with PBS, (b) nanofibrous sample sterilized with ethylene oxide without preliminary rinsing with PBS, (c) non-sterilized nanofibrous sample preliminary rinsed with PBS. Each point represents mean ± SD, n=3.

2.2.6 Dissolution of fibrous samples

The analysis revealed no content of alaptide trapped in the fibers after 14-day release experiment. Except for the one non-sterilized sample (replicate) with 1 wt.% loading, where ~6% of initial loading was determined, and also around 12% were determined in two replicate 2.5 wt.% loaded samples.

Some amount of not dissolved particles was observed after dissolution. These particles are assumed to be crystals of PBS salts, which had accumulated on the surface of samples after drying.

Additionally, the actual alaptide loading was calculated from the data of drug content obtained for negative control samples. This content was subsequently compared with content predicted from the initial drug concentration in a polymer solution before electrospinning on simple assumption that all the solvent evaporates (see Tab. 5).

Tab. 5 Comparison of alaptide content found using GPC analysis and values calculated (predicted) from the drug concentration in the initial polymer dispersion

Alaptide loading within PCL electrospun mats [mg/g]			
	Found using GPC		**Calculated (predicted)**
	Mean	**SD (n = 2)**	
PCL Ala 0.1 wt.%	11.482	0.790	6.25
PCL Ala 1 wt.%	68.569	0.109	62.5
PCL Ala 2.5 wt.%	154.56	13.49	156.25

As can be seen in Tab. 5, the mean values of alaptide content found using GPC and the values which were calculated are very close for 1 and 2.5 wt.% drug loading, whereas for the 0.1 wt.% drug loading, the predicted (calculated content) is twice higher, than determined using GPC analysis.

It can be seen from *Tab. 6* that percentage of alaptide that was flushed out during preliminary rinsing gives almost 100% as a sum with released amount of alaptide. However, one can assume the general amount as a complete as GPC was not able to detect alaptide under 10%. Moreover, as mentioned above, some amount of alaptide was trapped in dissolved fibrous samples.

Rinsing (sterilization) in EtOh had the biggest standard deviation. Whereas, rinsing in PBS gave almost the same results every time.

Tab. 6 Comparison of amounts and percentage amounts of flushed out alaptide (n=3) in dependence on initial alaptide loading, sterilization method and rinsing solution.

Alaptide initial loading [wt. %]	**Alaptide content in original sample [mg]**	**Flushed out amount of Alaptide [mg]**	**Flushed out percentage of Alaptide [%]**
Sterilized by EtOX, rinsed in PBS			
0.1	0.611 ± 0.002	0.109 ± 0.008	17.746 ± 1.491
1	3.448 ± 0.068	1.564 ± 0.193	45.429 ± 6.419
2.5	7.001 ± 0.067	3.530 ± 0.453	49.787 ± 5.468
Non-sterilized, rinsed in PBS			
0.1	0.614 ± 0.008	0.251 ± 0.026	40.100 ± 4.228
1	3.503 ± 0.018	1.881 ± 0.285	53.735 ± 8.329
2.5	7.133 ± 0.123	2.697 ± 0.716	37.459 ± 9.783
Rinsed in Ethanol			
0.1	0.625 ± 0.004	0.248 ± 0.023	39.644 ± 3.957
1	3.496 ± 0.021	1.810 ± 0.161	51.789 ± 4.895
2.5	7.180 ± 0.042	5.054 ± 1.565	70.417 ± 21.945

2.2.7 Fitting of the curves to mathematical models

The release data of alaptide were fitted in the mathematical models described in the section 1.3.2, namely zero-order, first-order, Higuchi and Korsmeyer-Peppas. Indeed, due to the significant initial burst release of alaptide, and related biphasic character of the release profiles it was not appropriate to fit the whole release profile at once. Thus, two phases of the release profiles, i.e. burst release phase and post-burst phase, were fitted separately. The compliance of the fitting was determined by comparing the mean values of determination coefficient, R^2. The release constant *k* was determined from the most relevant fitting model, which was found to be the Higuchi model. Furthermore, as mentioned in the section 1.3.2, the Korsmeyer-Peppas model can be applied only for the first 60% of release, regardless the shape of the delivery device, so that it was possible to apply this model on to release data of non-rinsed sample with 0.1 wt.% loading. For the rest of the samples release percentage exceeded 60% within first 5 hours, resulting in the lack of insufficient amount of data points for relevant fitting. Finally, due to the fact that the values for rinsed samples are relative (see section 0), it was appropriate to apply the fitting only on release data of non-rinsed samples. The results of fitting are shown in the following tables.

Tab. 7 The results of fitting of the first phase of release (burst release, first 24 hours) to the different mathematical models. NR denotes non-rinsed sample; k denotes the release constant for Higuchi model. The most relevant values of determination coefficient are put in bold.

	R^2			**k**
Sample\Model	Zero-order	First-order	Higuchi	
0.1 % - EtO - NR	0.959	0.967	**0.997**	2.873
1% - EtO - NR	0.781	0.875	**0.892**	7.684
2.5% - EtO - NR	0.728	0.849	**0,851**	8.159

Tab. 8 The results of fitting of the second phase of release profile (after the burst) to the different mathematical models.

	R^2			**k**
Sample\Model	Zero-order	First-order	Higuchi	
0.1 % - EtO - NR	0.876	0.891	**0.960**	1.124
1% - EtO - NR	0.610	0.605	**0.758**	0.139
2.5% - EtO - NR	0.681	0.678	**0.818**	0.240

The release exponent *n* for the Korsmeyer-Peppas model was found to be 0.135, with R^2=0.995, for the non-rinsed 0.1 wt.% sample.

2.2.8 Results of test of cellular viability

The extracts of materials modified by alaptide did not cause any decrease in cellular viability. Measured values were in range of 90-105% of control cells. Extracts of electrospun PCL caused slight reduction of cell viability by 1 day extract (decrease up to 92%) and by 14-days extract (up to 77%). However, according to the ISO 10993-5 norm, cytotoxic effect is considered when viability decreased under 70% of control cells. Fig. 22 shows fluctuations of cellular viability for each sample.

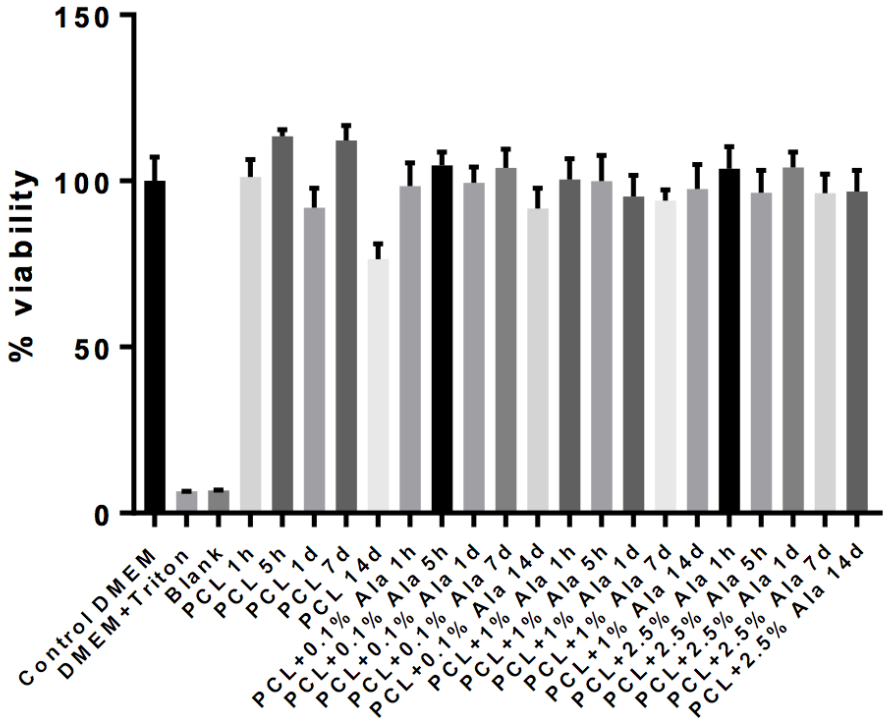

Fig. 22 Cell viability of fibroblasts exposed to a contact with material extracts during 14-days experiment (n=12).

2.3 Discussion

2.3.1 Contact angle measurement

The wettability or hydrophilicity of PCL electrospun nanofibrous layers was carried out by measuring a contact angle. As shown in Fig. 18 and Fig. 19, obtained values of dynamic contact angle were found to be lower for higher drug loadings. In other words, hydrophilicity of electrospun layers increased with increasing drug loading. The similar trend was reported earlier (Kadri, 2001), however for the swelling-controlled matrices. An increasing hydrophilicity of PCL with increasing amount of entrapped drug was also reported by Khandwekar *et al.* (2011). Fig. 19, also reveals that generally relationship between contact angle and drug loading is linear (R^2=0.895). Indeed, at highest used drug loading, i.e. 2.5 wt.%, PCL layers became hydrophilic with initial contact angle 67.16 ± 16.11°, whereas at 1 wt.% loading it is just in the middle between "hydrophobic" and "hydrophilic" according to definition (Förch, Schönherr and Jenkins, 2009), with initial contact angle 86.02 ± 11.70°, although, in fact, absorption of the droplet proceeds fast involving immediate contact angle decrement.

The contact angles obtained for the control sample (0 wt.% alaptide) and for the lowest drug loading (0.1 wt.%), i.e. 116.22 ± 26.83° and 126.76 ± 3.67° respectively, were consistent with values obtained by Luong-Van *et al.* (2006) for pure PCL nanofibers and PCL loaded with heparin (139 ± 6° and 132 ± 7°, respectively). Furthermore, the consistent values were reported by Kosorn *et al.* (2012) for PCL porous scaffolds before a plasma treatment (129.97 ± 0.40°). Nevertheless, one can found number of studies reporting the contact angle values around 80°, e.g. Khandwekar *et al.*, reported (2011) 78.58 ± 1.0° for porous scaffolds with entrapped heparin. Luong-Van *et al.* (2006) suggests that higher values could be caused by air trapped in material pores. However, it is more likely to result mainly from nano- or macroroughness of the material, which could be caused, for instance, by the surface of the spunbond substrate. Moreover, there is number of parameters within contact angle measurement, which could cause deviations. For instance, as suggests (Kadri, 2001), contact angle could be influenced by the droplet size – the larger drop may result in higher contact angle. However, this allegation can be partially refuted by the fact that in current study droplet size was 15 µL, likewise, in already mentioned study Luong-Van *et al.* (2006) with similar, but still higher values of contact angles, a droplet size was 10 µL. Meanwhile, Kalu *et al* (2016) used significantly

smaller droplet volume, i.e. 1 µL, and obtained slightly lower although still consistent values. It is also can be assumed, that electrostatic charge arising during handling of the layers might affect the contact angle values.

The fact that the droplet behavior was different at different spots of the layer could be explained by heterogeneity of both the electrospun structure (mainly fiber diameters) and drug distribution within the layers.

Additionally, the trend of linear decrement of the contact angle corresponds to almost linear decrement of the fiber diameter with the increasing drug loading, despite four concentrations (0, 0.1, 1 and 2.5 wt.%) are insufficient to search for a correlation.

2.3.2 *In Vitro* release of alaptide

Generally, the release profile of alaptide from each electrospun layer was biphasic (see *Fig. 20*), with a considerable initial burst release and subsequent slow sustained release. Huang and Brazel (2001) in their broad review reported a number of parameters causing a burst release in matrix-based devices. Generally, these parameters can be divided into several groups, among which are, for instance, processing conditions, surface characteristics and sample geometry. On the basis of observations on SEM images, release profile graphs and Huang and Brazel's review, it can be suggested, that two main reasons of burst release in current study was due to a) alaptide particles trapped on the surface due to high loadings, and b) migration of the drug to the surface during drying and storage of the layers after fabrication process (see Fig. 23). Both drug migration and entrapping of drug on the close to the surface lead to a similar situation, when drug particles on the surface have a short diffusional path, meanwhile it takes much longer for particles close to the center to diffuse out of a fiber.

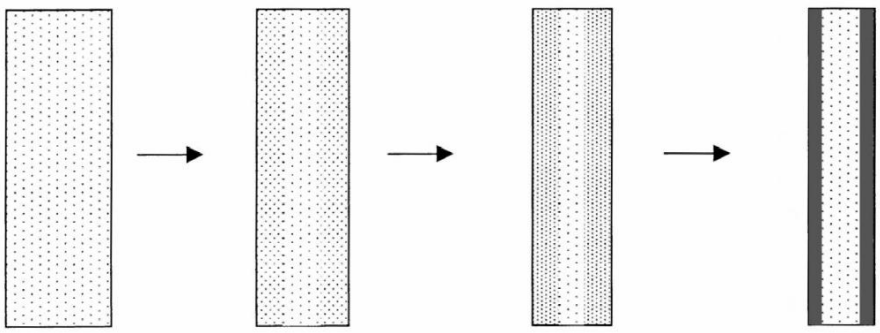

Fig. 23 Probable redepositing of a drug within a electrospun layer caused by convection during the drying (Huang and Brazel, 2001)

In addition, it is reasonable to assume, that diffusion of a drug proceeds faster from a fiber of a smaller diameter in comparisonn with thicker fibers. As was discussed before, increament of drug loading caused narrowing of fiber diameters range (see *Fig. 14* and *Tab. 3*) within 95% CI interval of <274.7; 343>. In other words, with increasing drug content, decreased amount of thicker fibers, leading to faster release of a drug. Finally, as could be seen in section 2.3.1, higher drug loading led to higher wettability of PCL electrospun layers. Thus, assuming this and also observations during 14-day experiments, it can be claimed that it took longer for the layers with lower drug loadings to get wet, which in turn means that delayed directed interaction between alaptide and the release medium, i.e. PBS (pH 7.4) solution. In other words, this factor could delay the drug release. Also, the increasing hydrophilicity could increase significance of further release mechanisms, e.g. swelling, that is normally not common (Siepmann, Siegel and Rathbone, 2012) for hydrophobic devices. These mechanisms could accelerate release rate, as well.

As previously discussed in section 2.2.5, drug release rate increased with increasing of initial drug loading. Considering cumulative percentage of released alaptide from non-rinsed samples, it can be seen that 34.33 ± 2.41% released within first 24 hours for 0.1 wt.% loading, whereas 77.74 ± 1.16% and 82.52 ± 1.68% was released for 1 wt.% and 2.5% respectively. Furthermore, considering overall amount of alaptide released within 14 days, only 49.08 ± 2.57% was released for 1 wt.%, while 79.49 ± 0.17% and 85.57 ± 1.80% was released for 1 wt.% and 2.5% respectively.

Similarly, as in case of burst release, the general release profile of alaptide could be affected by presence of fibers of different radii. Fig. 14 shows that the layer with 0.1 wt.% loading had the widest distribution of fibers. In other words, there was bigger number of thick fibers, which could slow down the release rate.

In addition, the layer with 0.1 wt.% loading was the only layer fabricated without adding a surfactant, i.e. SLS, in original polymer solution. Varma *et al.* (2004) in their review discussed an effect of surfactants on release rates of drug from matrix-based systems due to change in its wettability. According to Varma *et al.*, diffusion process could be divided into three main stages. Firstly, the wetting of the delivery device, which opens an access for a medium.; then dissolution of a drug within hydrated areas of the device; at the end, diffusion of dissolved drug through the matrix towards the release medium. Moreover,

the water uptake is affected not only by the porosity of the divice but also by wetability of individual pores.Varma *et al.* (2004) mentions Nokhodchi *et al.* (2002) who studied an effect of different surfactants on release rates. In their study it was reported that release rate of propranolol decreased as the concentration of SLS increased, suggesting that SLS is able to form complex with propranolol. Despite this, content of SLS within layers with 1 and 2.5 wt.% loading was probably too small, i.e. 0.75 mg/g, to significantly cause release rates.

Fig. *20* reveals that there was irrelevant difference between the release rates of non-sterilized samples and samples sterilized with EtO for 1 and 2.5 wt.% loadings. Moreover, this difference decreased with increasing drug loading. Although, for 1 wt.% loading, the release rates are slightly faster in case of sterilized samples, and for 0.1 wt.% this rate difference is even more considerable. Further, overall released amount of alaptide was slightly greater for sterilized samples, i.e. 33.55 ± 0.83% against 23.36 ± 2.04% for 0.1 wt.% and 45.26 ± 4.10% against 40.44 ± 0.55% for 1 wt.%. There is number of contrasting publications concerning EtO post-sterilization effects on biodegradable scaffolds and drug delivery devices, unfortunately, though very few publications concerning electropun devices can be found. Despite mostly changes affect the mechanical properties and biocompatibility, there are studies that reported significant change in morphology of polymer delivery device and even change in drug release profiles. For instance, Hsiao *et al.*, (2012) studied the effects of EtO sterilization on the release of an antibiotic, namely vancomycin from PLGA scaffold. It was reported that sterilized scaffolds did not performed any burst release in comparison with untreated samples. In addition, the total drug-releasing period for the EtO-treated samples was much shorter in comparison with non-sterilized samples. Finally, the overall amount of released antibiotic was less, as well. The results obtained in current study are consistent with the study by Horakova *et al* (2017) in the sense that EtO sterilization treatment was not found to influence fibrous morphology of the electrospun PCL samples. However, it is speculative to proof consistence with Hsiao's results in the sense of increment of drug release rate and overall amount of release drug. Dai *et al.* (2016) in their review, cited the example of number of studies reporting diametrically opposite results of EtO treatment.

Tab. *6* revealed that approximately a half of initial drug content was washed before the release experiment during the preliminary rinsing in PBS (pH 7.4) solution. Initially, it was expected to reduce a burst effect as it should have remove (dissolve) drug particles

on and near the surface of electrospun layers. However, even after rinsing in PBS solution, burst effect remained considerable, which was probably caused mainly by a migration of the drug particles (see Fig. 23). Thus, in next studies it is recommended to provide analysis of drug particle distribution within the electospun layers, e.g. via fluorescent labeling as was done in study by Luong-Van *et al.* (2006). Furthermore, Tab. 6 revealed that summing of the drug content flushed out by rinsing and the drug content released after 14 days, yields almost 100% of initial drug content for 1 and 2.5 wt.% loadings, i.e. appx. 91 and 94% respectively for sterilized samples; and appx. 95 and 92% for non-sterilized samples. However, sum of the flushed and released alaptide content for 0.1 wt.% loading differs, i.e. 52% for sterilized samples and 63% for non-sterilized samples. Comparing overall released amount after 14 days, it can be seen that in case of non-rinsed samples overall amount released is appx. 10% less than for rinsed samples. This could probably be explained by more complete wetting of samples by rinsing. Whereas non-rinsed samples due it high hydrophobicity could partially remain "un-wetted" and thus not completely immersed in PBS solution, thereby reducing potential releasing surface of the electrospun layer.

Mathematical fitting of release data revealed that the release profiles fitted the Higuchi model the best for both phases of release (burst phase and post-burst), suggesting diffusional release from a device. Moreover, within the burst release phase, the release constant *k*, calculated using the Higuchi model, was found to increase with the increasing drug loading, which in turn corresponds with the diffusion equation which assumes an increment in diffusion rate with increasing concentration gradient. However, for the post-burst phase, no trend for the release constant was observed. Additionally, the release exponent from the Korsmeyer-Peppas model was found to be 0.135 (<0.45) for the non-rinsed 0.1 wt.% sample, providing further support for assumption of the Fickian diffusion or quasi-Fickian diffusion mechanism dominance. This finding for *n* value was in agreement with the study by (Natu, de Sousa and Gil, 2010) for 50/50 PCL/poly(oxyethylene-b-oxypropylene-b-oxyethylene) bicomponent fibers loaded with timolol maleate. As suggest Xie and Wang, (2006), distinction of *n* values among other issues can be affected by the geometry of the electrospun layers and the fact that not all the fibers surfaces were in contact with the release medium. Nevertheless, the mechanism responsible for the sustained release after an initial burst effect remains unclear.

2.3.3 Morphology of samples after the experiment

Investigation of the electrospun layers after the experiment revealed that the changes in morphology were caused mainly by the release of alaptide rather than incubation in release medium itself, as the morphology of control samples did not remarkably change. On the other hand, it is important to mention, that 30-minutes sterilization (rinsing) by EtOH cause similar morphological changes as 14-days incubation in PBS solution. Moreover, the changes in morphology were more evident with the increasing drug loading. Taking into account that solubility of alaptide in water is almost the same as in ethanol (Dragicevic and Maibach, 2017) and the fact that 30-minute rinsing in ethanol washed out almost the same amount as 30-minute PBS rinsing, it is possible to assume that rapid dissolution of the drug was not the driven factor of morphology change. Probably, the difference between morphological behavior of the electrospun layers corresponds with its wettability. As was discussed above, the control samples had high contact angle, whereas the samples with higher drug loadings were found to be more hydrophilic. This suggests, that the samples with higher loadings were wetted more completely, resulting in more significant morphological changes. Furthermore, the fact that EtOH has lower surface tension and is able to wet PCL layers within shorter period of time, provides further support of this assumption.

Additionally, on the SEM images of the electrospun layers after the release experiment were observed small particles (~15 μm), which were assumed to be crystals of PBS salts adsorbed to the surface after drying. This assumption is also supported by the weight gain of the samples after the end of the experiment and also by the fact that after complete dissolving the fibrous samples, white crystal-like sludge particles appeared on the bottom of the vials. The experimental attempt to quantify these crystals revealed that its amount increased with increasing drug loading, i.e. 2.93% for the control sample and 9.02% for 2.5 wt.% drug loaded sample. Unfortunately, no studies reporting this issue were found.

2.3.4 Dissolution of fibrous samples

Dissolution of the electrospun layers revealed that actually the complete alaptide was released within 14 days for all the 1 and 2.5 wt.% samples, except for the one non-sterilized sample (replicate) with 1 wt.% loading, where ~6% of initial loading was determined, and also around 12% were determined in two replicate 2.5 wt.% loaded samples. However, it is assumed that GPC was not able to correctly detect entrapped alaptide under 5%. These findings were consistent with the study by (Natu, de Sousa and

Gil, 2010), where approximately 10% of drug was entrapped in PCL fibers with higher drug loadings. According to Natu (2010), this entrapped drug fraction might be located in crystalline areas of the fibers, i.e. inaccessible for water. Thus, diffusion and desorption of this drug was possible only after polymer degradation, whose effect is though negligible within 14 days of the experiment (Ravi Kumar, 2016). Surprisingly, no alaptide content entrapped in 0.1 wt.% samples was found. Even though the overall cumulative release values were significantly lower than 100%.

Moreover, dissolution of the fibrous samples revealed the actual drug loading [mg/g]. Actual values were found to be close to the predicted values for 1 and 2.5 wt.% samples, which in turn indicates of homogeneous distribution of the drug within the layers, despite all the discussed factors supporting the contrary. On the other hand, the actual drug loading value for 0.1 wt.% sample was found to be almost twice as much as the predicted value, which can be explained either insufficient precision during preparation of the polymer suspensions or significant heterogeneity of the alaptide distribution within the layers.

2.3.5 Influence of extracts of the materials on cellular viability

Assessment of cytotoxity of materials extracts was carried out for each drug loadings and for the control sample. The extracts of materials modified by alaptide did not cause any decrease in cellular viability. Measured values were in range of 90-105% of control cells. Extracts of electrospun PCL caused slight reduction of cell viability by 1 day extract (decrease up to 92%) and by 14-days extract (up to 77%). However, according to the ISO 10993-5 norm, cytotoxic effect is considered when viability decreased under 70% of control cells.

Nevertheless, test of cell proliferation on the materials was not successful and was not mentioned in the results section. Cells did not grow even on the control samples without alaptide, which could be caused by residuals of EtO due to insufficient airing of the samples. Moreover, cells growth could be caused also by the addition of surfactant (SLS), which, might change surface properties of the samples.

2.4 Conclusion

To date, an exploration of electrospun nanofiber-based drug delivery systems is still in the very early stage and handful of related studies can be found. However, this field of research continuously gets more and more attention due to its great potential. The aim of this study was to design an experimental method for investigation of drug release kinetics from electrospun nanofibrous layers. Also, the aim was to assess obtained release kinetics and compare it with the results found in the literature.

First of all, the drug-loaded polycaprolactone layers of nanofibrous electrospun nanofibers were successfully fabricated using electrospinning technology. A spirocyclic synthetic dipeptide, namely alaptide, was used as a model drug. A 16 wt.% PCL solution in 9:1 chloroform/ethanol was used to prepare the spinning polymer solution, into which alaptide in amount of 0.1, 1 and 2.5 wt.% was added to obtain drug-loaded spinning polymer solutions. The obtained nanofibrous layer were found to be heterogeneous with wide range of diameters distribution. The fiber diameter range was narrowing with the increasing drug loading. The thinnest fibers (308.87 nm, <275; 343> nm) were achieved from solution with the highest loading of alaptide (2.5 wt. %). The measurement of a contact angle revealed the linear increase of hydrophilicity of the layers with the increasing drug loading. The initial contact for a control layer was 116.22 ± 26.83° and for the highest drug loading it decreased to 67.16 ± 16.11°. *In vitro* tests of cytotoxicity of material extracts revealed that even the highest used alaptide loading did not cause decrement of cell viability below the allowable level.

Three factors affecting morphology and drug release kinetics in vitro were investigated, namely an effect of sterilization with ethylene oxide (EtO) or ethanol (EtOH), an effect of preliminary rinsing in PBS solution and finally an effect of drug loading capacity. The release profiles for each electorspun layer were biphasic, consisting of an initial burst release within first 24 hours and further slow sustained release for the remaining 13-days period, suggesting heterogeneous drug distribution within the electrospun layers. The release alaptide amount within the burst release was increasing with increasing drug loading. The preliminary rinsing in PBS solution was found to wash out ~50% of initial drug content, which, however, did not reduce a burst effect. The significant changes of morphology of the electrospun layers were observed after the release of higher drug loadings. These morphology changes involved increment of smoothness of the surface

and relaxation of individual fibers. Also, an adsorption of PBS crystals on the surface of the layers were observed after the experiment. Its quantification revealed that the amount of these particles increased with increasing drug loading and reached ~10% of the original weight for 1 and 2.5 wt.% loadings. The sterilization by EtO did not cause any remarkable changes in the morphology of the layers, however differences on release profiles were observed. Particularly, release rate for sterilized samples was slightly faster. This release rate difference was decreasing with the increasing drug loading, so that for the 2.5 wt.% loading it was irrelevant. Whereas the sterilization by EtOH was found to lightly affect the surface morphology of the layers, leading to higher smoothness. The drug percentage amount which was flushed out by EtOH was consistent with the amount flushed out by PBS for 0.1 and 1 wt.% loadings. Whereas it was almost twice time higher for the 2.5 wt.% loading, even thou standard deviation was higher. The comparison of obtained data with existing mathematical models was complicated due to a biphasic nature of release profiles, particularly due to a significant burst release for the higher drug loadings. However, separate fitting of both burst-phase and post-burst phase revealed that the release profiles fit the Higuchi model the best, suggesting the dominance of simple diffusion mechanism of the release.

Nevertheless, there are still many challenges and limitations remaining. In particular, the numerical determination of diffusivity of alaptide turned out to be more complicated after more detailed investigation, due to the problem of boundary between the two phases. Indeed, the study of diffusion equation and determination of diffusivities will be continued in the dissertation thesis. In any case, the design of the experiment which was established in this study was found to be stable and descriptive. Thus, bearing in mind the results obtained in current study, this methodology might be successfully used in further studies. Additionally, it is reasonable to assume that obtained materials could be used as a modification of yet existing wound dressing product, i.e. NANOTARDIS.

2.5 References

'Biological evaluation of medical devices -- Part 5: Tests for in vitro cytotoxicity' (2009). International Organization for Standardization. Available at: https://www.iso.org/standard/36406.html (Accessed: 1 April 2018).

Brown, R. (1828) 'XXVII. A brief account of microscopical observations made in the months of June, July and August 1827, on the particles contained in the pollen of plants; and on the general existence of active molecules in organic and inorganic bodies', *The Philosophical Magazine*. Taylor & Francis, 4(21), pp. 161–173. doi: 10.1080/14786442808674769.

Caretto, L. (2016) *Solution of the Diffusion Equation*. Available at: http://www.csun.edu/~lcaretto/me501b/diffusion.doc.

Chasin, M. and Langer, R. (1990) *Biodegradable Polymers as Drug Delivery Systems*. New York: M. Dekker (Drugs and the Pharmaceutical Sciences). Available at: https://books.google.cz/books?id=gmlUPNSW36oC.

Chicone, C. (2017) *An invitation to applied mathematics with differential equations*. Amsterdam: Academic Press.

Crank, J. (1975) *the Mathematics of Diffusion*. 2nd edn. London: Oxford University Press.

Dai, Z. *et al.* (2016) 'Sterilization techniques for biodegradable scaffolds in tissue engineering applications.', *Journal of tissue engineering*. SAGE Publications, 7, p. 2041731416648810. doi: 10.1177/2041731416648810.

Dash, S. *et al.* (2010) 'Review Kinetic Modeling on Drug Release from Controlled Drug Delivery Systems', *Acta Poloniae Pharmaceutica-Drug Research*, 67(3), pp. 217–223.

Dash, T. K. and Konkimalla, V. B. (2012) 'Poly-ε-caprolactone based formulations for drug delivery and tissue engineering: A review', *Journal of Controlled Release*. Elsevier B.V., 158(1), pp. 15–33. doi: 10.1016/j.jconrel.2011.09.064.

Dragicevic, N. and Maibach, H. I. (2017) *Percutaneous Penetration Enhancers Chemical Methods in Penetration Enhancement Modifi cation of the Stratum Corneum*. doi: 10.1007/978-3-662-53273-7.

Einstein, A. (1905) ‘Über die von der molekularkinetischen Theorie der Wärme geforderte Bewegung von in ruhenden Flüssigkeiten suspendierten Teilchen’, *Annalen der Physik*. Wiley-Blackwell, 322(8), pp. 549–560. doi: 10.1002/andp.19053220806.

Fick, A. (1855) ‘Ueber Diffusion’, *Annalen der Physik*. Wiley-Blackwell, 170(1), pp. 59–86. doi: 10.1002/andp.18551700105.

Förch, R., Schönherr, H. and Jenkins, A. T. A. (2009) *Surface Design: Applications in Bioscience and Nanotechnology*. Wiley. Available at: https://books.google.cz/books?id=cvn5l-QytVIC.

Gamow, G. (1988) *One, two, three-- infinity : facts and speculations of science*. New York: Dover Publications.

Grassi, M. and Grassi, G. (2014) ‘Application of mathematical modeling in sustained release delivery systems.’, *Expert opinion on drug delivery*, 11(8), pp. 1299–321. doi: 10.1517/17425247.2014.924497.

Gurevich, S. V. (2008) *Numerical methods for complex systems*. University of Münster. Available at: https://www.uni- muenster.de/Physik.TP/archive/typo3/fileadmin/lehre/NumMethoden/PDE2.pdf.

Higuchi, T. (1963) ‘Mechanism of sustained-action medication. Theoretical analysis of rate of release of solid drugs dispersed in solid matrices’, *Journal of Pharmaceutical Sciences*, 52(12), pp. 1145–1149. doi: 10.1002/jps.2600521210.

Hillery, A. M., Lloyd, A. W. and Swarbrick, J. (2001) *Drug delivery and targeting for pharmacists and pharmaceutical scientists*. London: Taylor & Francis. Available at: https://www.dawsonera.com/guard/protected/dawson.jsp?name=https://shib-idp.ucl.ac.uk/shibboleth&dest=http://www.dawsonera.com/depp/reader/protected/external/AbstractView/S9780203302767.

Holowka, E. P. and Bhatia, S. K. (2014) ‘Controlled-Release Systems’, in *Drug Delivery*. New York, NY: Springer New York, pp. 7–62. doi: 10.1007/978-1-4939-1998-7_2.

Horakova, J. *et al.* (2017) ‘Effect of ethylene oxide sterilization on electrospun vascular grafts made from biodegradable polyesters’, submitted to: *Materials Science and Engineering: C*.

Hrib, J. *et al.* (2015) 'Nanofibers for drug delivery - Incorporation and release of model molecules, influence of molecular weight and polymer structure', *Beilstein Journal of Nanotechnology*, 6(1), pp. 1939–1945. doi: 10.3762/bjnano.6.198.

Hsiao, C.-Y. *et al.* (2012) 'The influence of γ irradiation and ethylene oxide treatment on the release characteristics of biodegradable poly(lactide-co-glycolide) composites', *Polymer Degradation and Stability*. Elsevier, 97(5), pp. 715–720. doi: 10.1016/J.POLYMDEGRADSTAB.2012.02.015.

Huang, X. and Brazel, C. S. (2001) 'On the importance and mechanism of burst release in matrix controlled drug delivery systems.', *Journal of Controlled Release*, 73, pp. 121–136.

Jampilek, J. *et al.* (2014) 'Alaptide : Methods of effecting its solubility,membrane permeation and pharmaceutical compositions for human and/or veterinary applications'. Available at: https://patentscope.wipo.int/search/en/detail.jsf?docId=WO2014019556&recNum=1&maxRec=&office=&prevFilter=&sortOption=&queryString=&tab=PCTDescription (Accessed: 14 March 2018).

Jiang, H. *et al.* (2005) 'A facile technique to prepare biodegradable coaxial electrospun nanofibers for controlled release of bioactive agents', *Journal of Controlled Release*, 108(2–3), pp. 237–243. doi: 10.1016/j.jconrel.2005.08.006.

Julínek, O. *et al.* (2010) 'Product of alaptide synthesis: Determination of the absolute configuration', *Journal of Pharmaceutical and Biomedical Analysis*, 53(4), pp. 958–961. doi: 10.1016/j.jpba.2010.07.007.

Kadri, B. V. (2001) *Mechanism of Drug Release From Matrix Tablets Involving Moving Boundaries*. University of Toronto. Available at: https://tspace.library.utoronto.ca/bitstream/1807/16014/1/MQ63184.pdf.

Kalu, S., Ufere, J. and Sultana, N. (2016) 'Contact Angle, Conductivity and Mechanical Properties of Polycaprolactone/Hydroxyapatite/Polypyrrole Scaffolds Using Freeze-Drying Technique', 11(23), pp. 13686–13691. Available at: www.arpnjournals.com.

Karimi, M. (2011) 'Diffusion in Polymer Solids and Solutions', in Markoš, J. (ed.) *Mass Transfer in Chemical Engineering Processes*. Rijeka: InTech. doi: 10.5772/23436.

Kenawy, E. R. *et al.* (2002) 'Release of tetracycline hydrochloride from electrospun poly(ethylene-co-vinylacetate), poly(lactic acid), and a blend', *Journal of Controlled Release*, 81(1–2), pp. 57–64. doi: 10.1016/S0168-3659(02)00041-X.

Khandwekar, A. P. *et al.* (2011) 'Surface Engineering of Polycaprolactone by Biomacromolecules and their Blood Compatibility', *Journal of Biomaterials Applications*. SAGE PublicationsSage UK: London, England, 26(2), pp. 227–252. doi: 10.1177/0885328210367442.

Kojic, M. *et al.* (2017) 'A radial 1D finite element for drug release from drug loaded nanofibers', *Journal of the Serbian Society for Computational Mechanics*, 11(1), pp. 82–93. doi: 10.24874/jsscm.2017.11.01.08.

Kosorn, W. *et al.* (2012) 'Surface Modification of Polycaprolactone Scaffolds by Plasma Treatment for Chondrocyte Culture'. doi: 10.7763/IPCBEE.

Luong-Van, E. *et al.* (2006) 'Controlled release of heparin from poly(ε-caprolactone) electrospun fibers', *Biomaterials*, 27(9), pp. 2042–2050. doi: 10.1016/j.biomaterials.2005.10.028.

Mehrer, H. and Stolwijk, N. (2009) 'Heroes and Highlights in the History of Diffusion', *Diffusion Fundamentals*, 11(1), pp. 1–32. Available at: http://ul.qucosa.de/fileadmin/data/qucosa/documents/18859/diff_fund_11%282009%291.pdf.

Nakielski, P. *et al.* (2015) 'Experimental and numerical evaluation of drug release from nanofiber mats to brain tissue', *Journal of Biomedical Materials Research - Part B Applied Biomaterials*, 103(2), pp. 282–291. doi: 10.1002/jbm.b.33197.

Nakielski, P., Kowalczyk, T. and Kowalewski, T. A. (2013) 'Modeling Drug Release from Materials Based on Electrospun Nanofibers', in *COMSOL conference*. Rotterdam, p. 6. Available at: http://www.ippt.pan.pl/Repository/o2265.pdf.

Natu, alina V, de Sousa, H. C. and Gil, M. H. (2010) 'Effects of drug solubility, state and loading on controlled release in bicomponent electrospun fibers', *International Journal of Pharmaceutics*. Available at: https://pdfs.semanticscholar.org/63d3/756633a130dc976f5300b5679fa10fe9d31d.pdf (Accessed: 22 February 2018).

Niraj *et al.* (2013) ‘Sustained and controlled drug delivery system - As a part of modified release dosage form’, *International Journal of Pharma Sciences*, 2(5), pp. 586–601.

Nokhodchi, A. *et al.* (2002) ‘The effect of various surfactants on the release rate of propranolol hydrochloride from hydroxypropylmethylcellulose (HPMC)-Eudragit matrices’, *European Journal of Pharmaceutics and Biopharmaceutics*. Elsevier, 54(3), pp. 349–356. doi: 10.1016/S0939-6411(02)00120-0.

Petlin, D. G. *et al.* (2017) ‘A fiber distribution model for predicting drug release rates’, *Journal of Controlled Release*, 258, pp. 218–225. doi: 10.1016/j.jconrel.2017.05.021.

Philibert, J. (2005) ‘One and a half century of diffusion: Fick, Einstein, before and beyond’, *Diffusion Fundamentals*, 4, pp. 1–19. Available at: http://ul.qucosa.de/fileadmin/data/qucosa/documents/19442/diff_fund_4%282006%296.pdf.

Qin, Y. (2015) *Medical Textile Materials*. Elsevier Science (Woodhead Publishing Series in Textiles). Available at: https://books.google.cz/books?id=wsPlBwAAQBAJ.

Ravi Kumar, M. N. V. (2016) *Handbook of polyester drug delivery systems*. 1st edn. New York: Pan Stanford.

Ritger, P. L. and Peppas, N. A. (1987) ‘A simple equation for description of solute release I. Fickian and non-fickian release from non-swellable devices in the form of slabs, spheres, cylinders or discs’, *Journal of Controlled Release*, 5(1), pp. 23–36. doi: 10.1016/0168-3659(87)90034-4.

Rossi, F., Perale, G. and Masi, M. (2016) *Controlled Drug Delivery Systems Towards New Frontiers in Patient Care*. Springer, Cham. doi: 10.1007/978-3-319-02288-8.

Siepmann, F. (2008) ‘Mathematical modeling of drug delivery’, *International Journal of Pharmaceutics*. Elsevier, 364(2), pp. 328–343. doi: 10.1016/J.IJPHARM.2008.09.004.

Siepmann, J., Siegel, R. A. and Rathbone, M. J. (2012) *Fundamentals and Applications of Controlled Release Drug Delivery*. Springer US (Advances in Delivery Science and Technology). Available at: https://books.google.cz/books?id=9yKSJdK37aMC.

Siepmann, J. and Siepmann, F. (2012) ‘Modeling of diffusion controlled drug delivery’, *Journal of Controlled Release*. Elsevier B.V., 161(2), pp. 351–362. doi:

10.1016/j.jconrel.2011.10.006.

Sultanova, Z. *et al.* (2016) ‘Controlled release of a hydrophilic drug from coaxially electrospun polycaprolactone nanofibers’, *International Journal of Pharmaceutics*. Elsevier B.V., 505(1–2), pp. 133–138. doi: 10.1016/j.ijpharm.2016.03.032.

Thomas, V. *et al.* (2006) ‘Mechano-morphological studies of aligned nanofibrous scaffolds of polycaprolactone fabricated by electrospinning.’, *Journal of biomaterials science. Polymer edition*, 17(9), pp. 969–84. Available at: http://www.ncbi.nlm.nih.gov/pubmed/17094636 (Accessed: 11 April 2018).

Varma, M. V. S. *et al.* (2004) ‘Factors Affecting Mechanism and Kinetics of Drug Release from Matrix-Based Oral Controlled Drug Delivery Systems’, *American Journal of Drug Delivery*, 2(1), pp. 43–57. doi: 10.2165/00137696-200402010-00003.

Xie, J. and Wang, C. H. (2006) ‘Electrospun micro- and nanofibers for sustained delivery of paclitaxel to treat C6 glioma in vitro’, *Pharmaceutical Research*, 23(8), pp. 1817–1826. doi: 10.1007/s11095-006-9036-z.

Yarin, A. L., Pourdeyhimi, B. and Ramakrishna, S. (2014) *Fundamentals and Applications of Micro and Nanofibers*. Cambridge University Press. Available at: https://books.google.cz/books?id=_KBcAwAAQBAJ.

Yu, D.-G. *et al.* (2009) ‘Electrospun nanofiber-based drug delivery systems’, *Health*, 01(02), pp. 67–75. doi: 10.4236/health.2009.12012.

Самарский, А. and Тихонов, А. (1999) *Уравнения математической физики*. изд.6-е, и. Москва: МГУ.

List of figures

List of tables